

New Phytologist Supporting Information

Article title: New fluorescent auxin probes visualize tissue-specific and subcellular distributions of auxin in *Arabidopsis*

Authors: Barbora Pařízková, Asta Žukauskaitė, Thomas Vain, Peter Grones, Sara Raggi, Martin Kubeš, Martin Kieffer, Simsa M. Doyle, Miroslav Strnad, Stefan Kepinski, Richard Napier, Karel Doležal, Stéphanie Robert, and Ondřej Novák

Article acceptance date: [Click here to enter a date.](#)

The following Supporting Information is available for this article:

Fig. S1 Library of fluorescent auxin analogues and scheme of screening strategy that was used for selecting the best candidates.

Fig. S2 Testing of the biological activity of the FluorA compounds in auxin-related bioassays.

Fig. S3 Concentration and time-dependent accumulation of selected FluorA compounds.

Fig. S4 Distribution of FluorA compounds *in planta*.

Fig. S5 Tissue-specific distribution response of FluorA II to light in apical hook.

Fig. S6 Subcellular localization of FluorA XI.

Table S1 Quantification of *Arabidopsis* primary root length after 5 days of treatment with FluorA compounds.

Table S2 Uptake and metabolization of FluorA compounds *in planta* determined by sensitive liquid chromatography–mass spectrometry (LC-MS) detection.

Table S3 LC-MS determination of 2,4-D uptake to *Arabidopsis* roots after treatment of *Arabidopsis* seedlings with increasing 2,4-D concentrations.

Table S4 Biological activity of FluorA compounds estimated by the quantification of Venus fluorescence signal of *p35S::DII-Venus Arabidopsis* seedlings in response to FluorA treatment.

Table S5 Effect of active auxin efflux on FluorA distribution in primary root.

Table S6 Effect of active auxin influx on FluorA uptake in primary root.

Methods S1 Synthesis of FluorA compounds.

Methods S2 LC-MS/MS determination of metabolization dynamics.

Methods S3 Surface plasmon resonance (SPR).

Methods S4 GUS assay.

Notes S1 Storage and usage of the compounds.

Dataset S1 Raw data obtained from Surface Plasmon Resonance (SPR) binding analysis of FluorA compounds to auxin receptor.

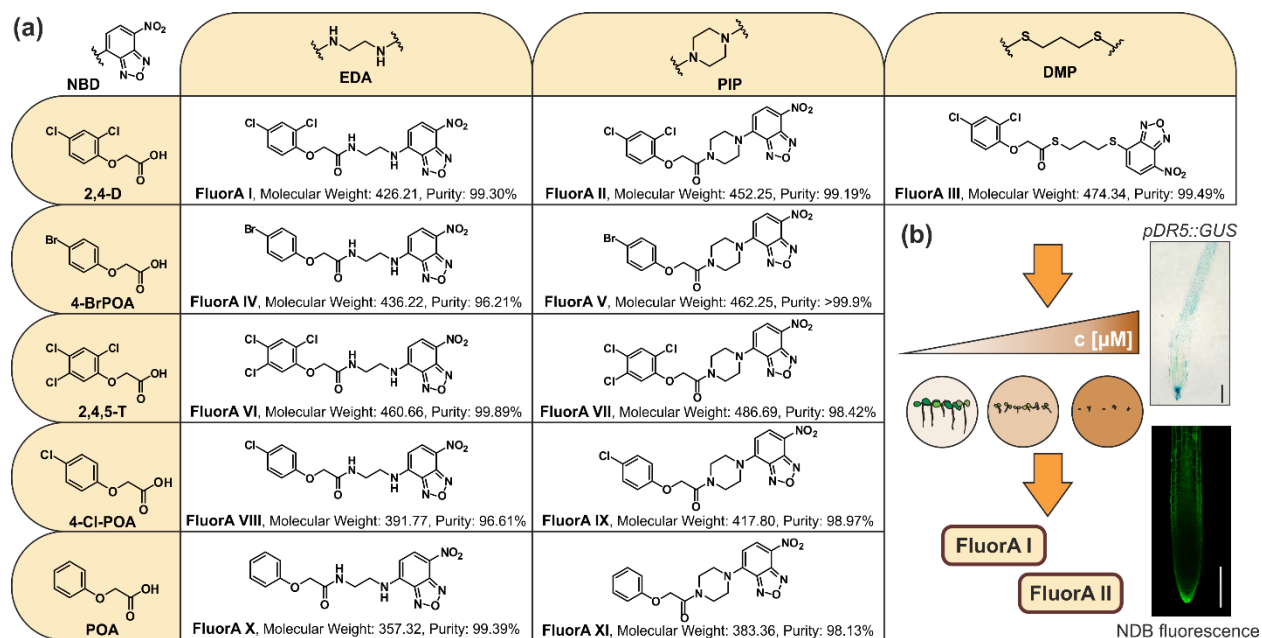


Fig. S1 Library of fluorescent auxin analogues and scheme of screening strategy that was used for selecting the best candidates. (a) The complete list of the FluorA (I-XI) compounds prepared for this study with their structures, molecular weights and purities including structures of the synthetic auxins 2,4-dichlorophenoxyacetic acid (2,4-D), 4-bromophenoxyacetic acid (4-Br-POA), 2,4,5-trichlorophenoxyacetic acid (2,4,5-T), 4-chlorophenoxyacetic acid (4-Cl-POA) and phenoxyacetic acid (POA), the ethylenediamine (EDA), piperazine (PIP) and 1,3-dimercaptopropene (DMP) linkers and the fluorescent label 7-nitro-2,1,3-benzoxadiazole (NBD) used. No free acids were detected in the stock solutions of the compounds. (b) Scheme of the screening strategy leading to selection of FluorA I and FluorA II. The compounds were evaluated according to their ability to reduce primary root growth of *Arabidopsis thaliana* Col-0 WT in a concentration-dependent manner and to induce *pDR5::GUS* expression in the root tip. In addition, the intensity of the NBD fluorescence signal in the root tip was assessed.

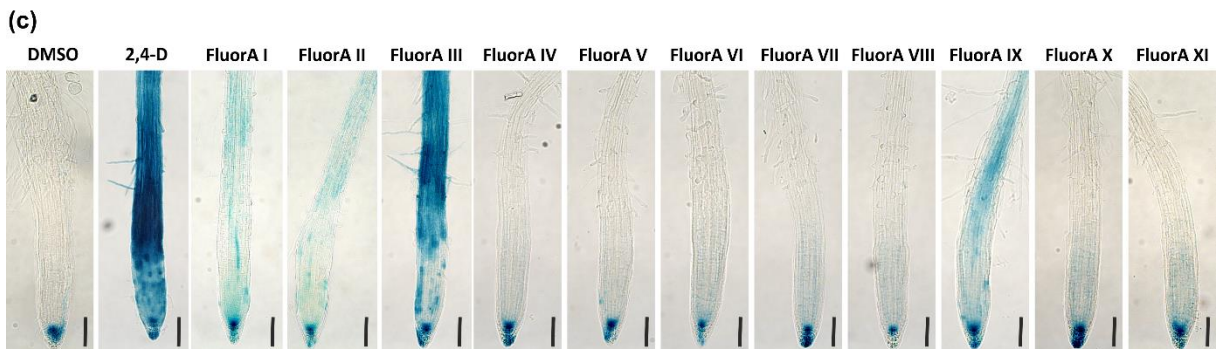
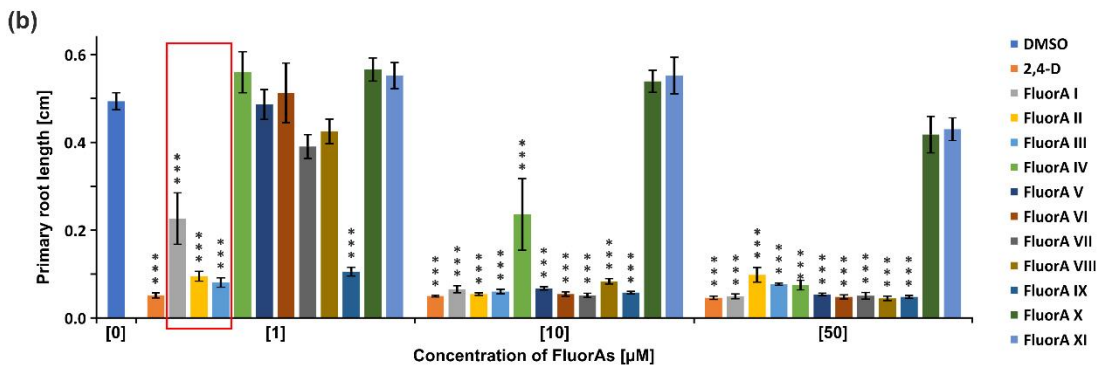
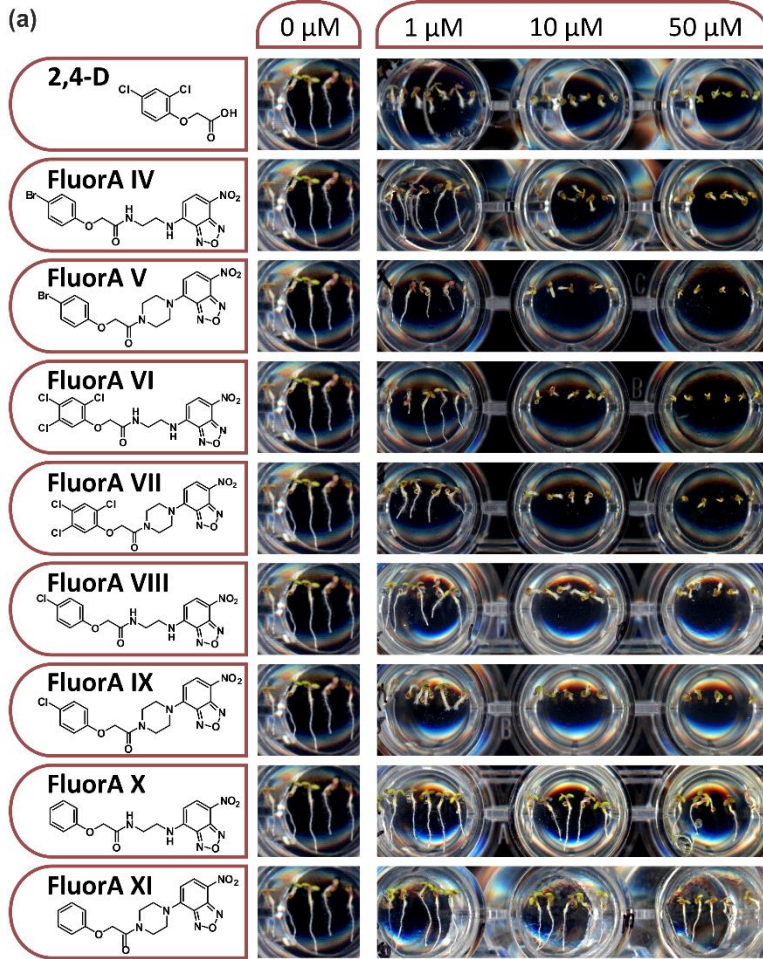


Fig. S2 Testing of the biological activity of the FluorA compounds in auxin-related bioassays. (a) Seedlings of *Arabidopsis thaliana* Col-0 WT were grown in the presence of dimethyl sulfoxide (DMSO) (0 μ M) or different concentrations of 2,4-dichlorophenoxyacetic acid (2,4-D) or FluorAs (1, 10, or 50 μ M) for five days. (b) Quantification of the primary root length of seedlings in (a). Statistical analyses were performed using the Student's t-test to compare to DMSO, values are means \pm SE (n=10 from 2 independent biological replicates). ***: p-value < 0.001. Red square shows the most active candidates selected from the screen. (c) Five-day-old seedlings of *Arabidopsis pDR5::GUS* marker line were treated with DMSO or with 10 μ M 2,4-D or FluorA compounds for 5 h and *DR5* expression in the primary roots was then examined by GUS (β -glucuronidase) staining. Scale bars represent 100 μ m.

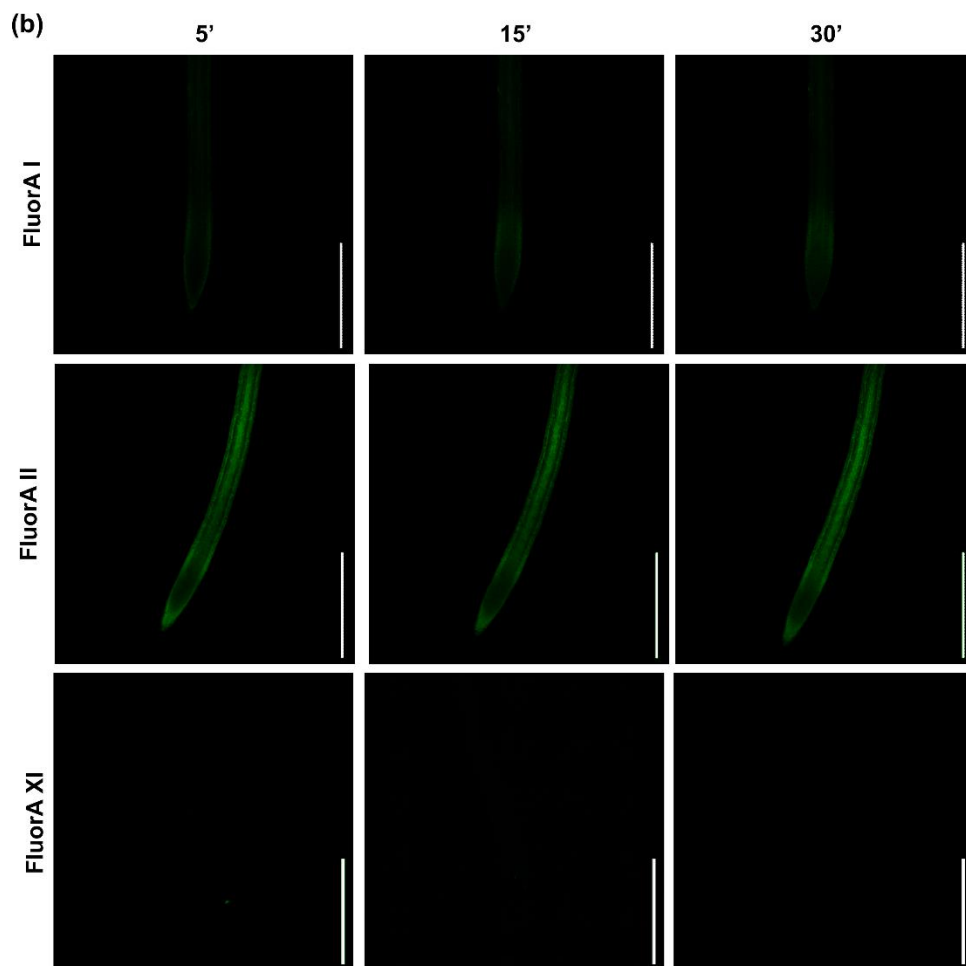
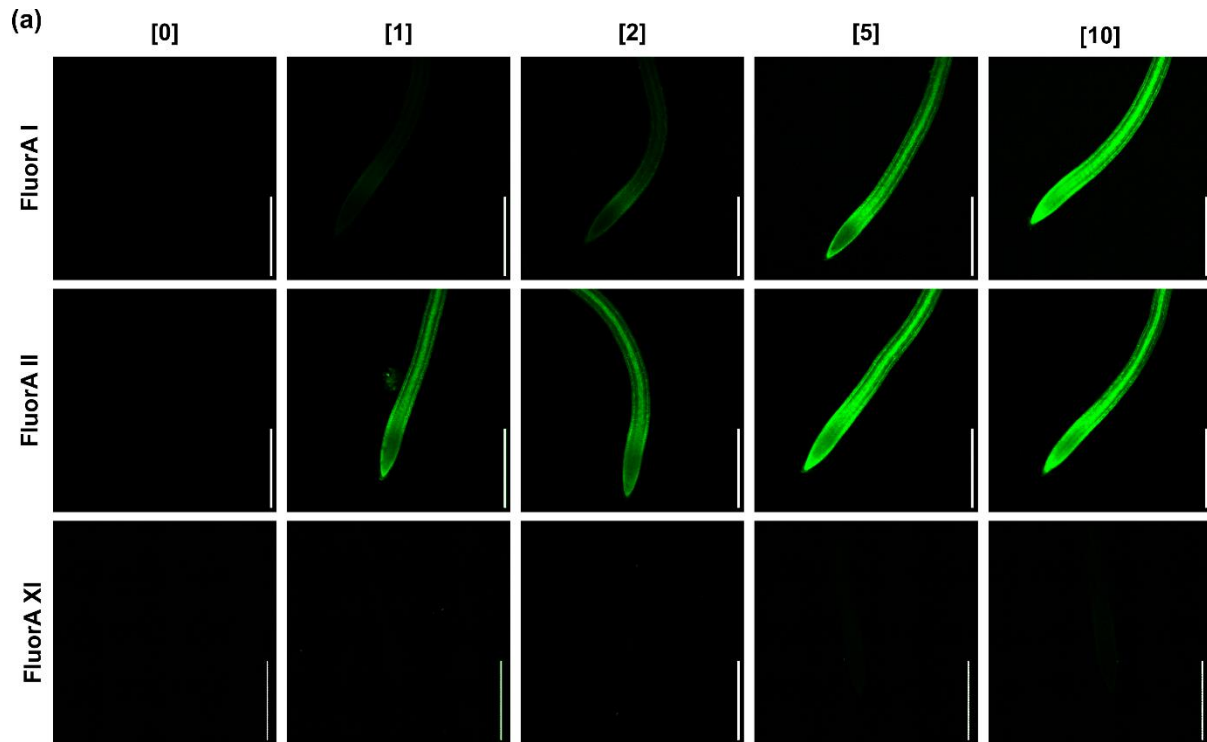


Fig. S3 Concentration and time-dependent accumulation of selected FluorA compounds. Five-day-old *Arabidopsis* Col-0 WT seedlings were treated in liquid medium at the indicated concentrations for 15 minutes (a) or treated with 2 μ M FluorAs or DMSO for 5, 15 or 30 minutes (b). Scale bar represents 500 μ m. The same confocal settings were used for all images, which were those optimized for FluorA II fluorescence.

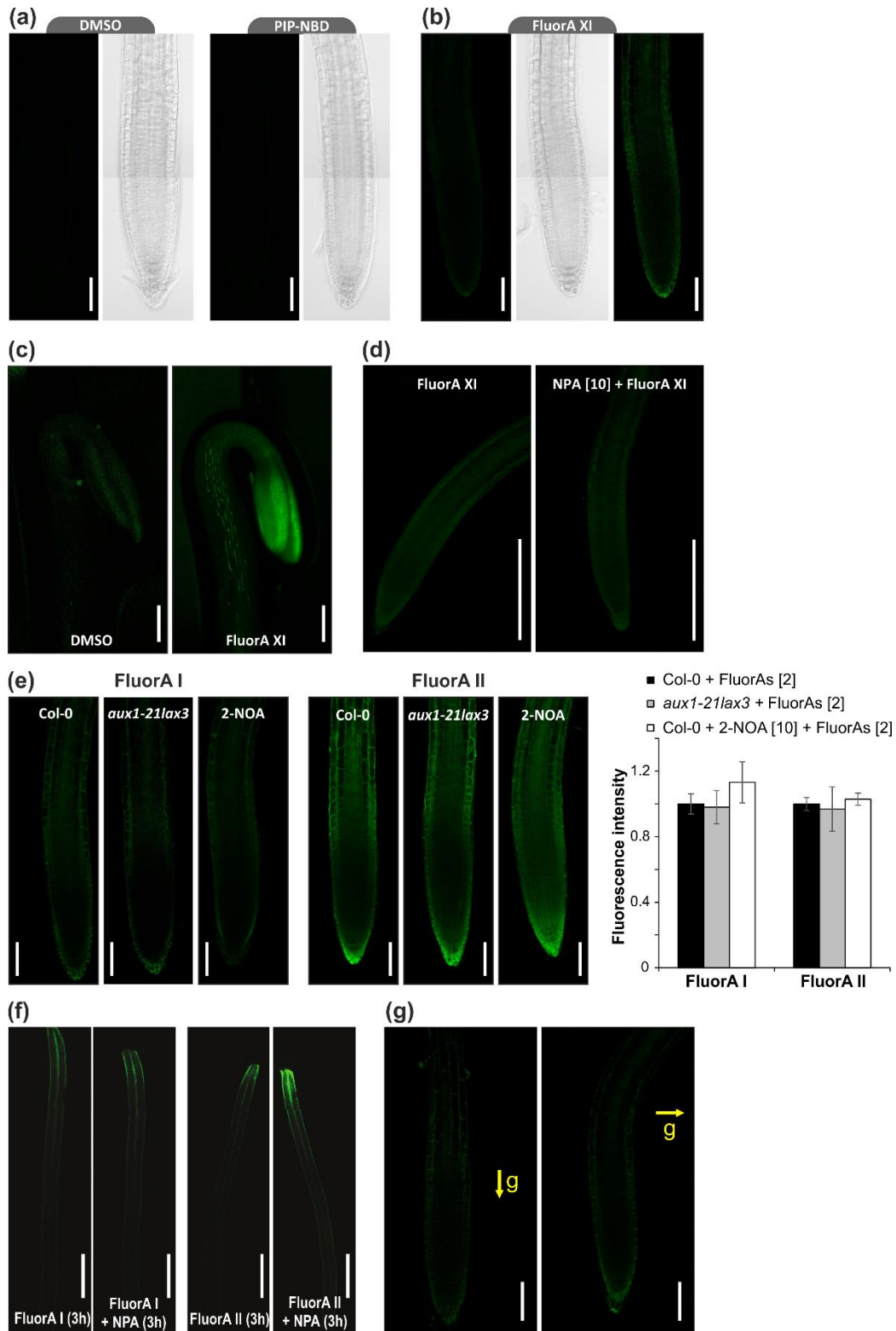


Fig. S4 Distribution of FluorA compounds *in planta*. (a,b) Weak fluorescent pattern of FluorA XI (a) and no fluorescent signal with piperazine - 7-nitro-2,1,3-benzoxadiazole (PIP-NBD) or DMSO control (b) in *Arabidopsis thaliana* Col-0 WT roots after optimized treatments (2 μ M, 15 min).

Scale bars indicate 100 μm . The fluorescent signal is shown without digital enhancement (a, left) and with digital enhancement (a, right) for FluorA XI to improve visibility. (c) Seedlings treated with 2 μM FluorA XI or equivalent volume of DMSO for 15 min. DMSO treatment showed no specific fluorescent output and FluorA XI did not exhibit differential accumulation in apical hooks of dark-grown *Arabidopsis* Col-0 WT seedlings. Scale bars indicate 1 mm. The fluorescent signal was digitally enhanced for FluorA XI to improve visibility. (d) *Arabidopsis* Col-0 seedlings were pre-treated in liquid medium with 10 μM NPA or DMSO for 3 hours before treating with 2 μM FluorA XI for 15 minutes. NPA pre-treatment did not promote FluorA XI accumulation. Scale bars indicate 300 μm (e) *Arabidopsis* Col-0 WT and *aux1-21lax3* seedlings were incubated with 2 μM FluorAs for 15 min. Col-0 seedlings were also pre-treated with 10 μM 2-naphthoxyacetic acid (2-NOA) for 3 h. No significant effect on fluorescence distribution or intensity of FluorAs was observed after disruption of auxin influx by these approaches. Statistical analyses were performed using the Student's *t*-test to compare to Col-0 without 2-NOA, values are means \pm SE ($n > 20$ from 3 independent biological replicates); no statistically significant differences were found. Scale bars indicate 100 μm . (f) Agar blocks with 2 μM FluorA compounds were placed on top of decapitated hypocotyls of three-day-old dark-grown *Arabidopsis* Col-0 WT seedlings and the basipetal transport of the compounds was monitored after 3 h. As a control, 3-hour pre-treatment with 10 μM *N*-1-naphthylphthalamic acid (NPA) was used to assess the contribution of diffusion. All treatments led to the accumulation of the fluorescent signal near the agar block, therefore NPA did not completely inhibit the transport of the FluorAs. Scale bars indicate 1 mm. (g) Gravistimulated roots of *Arabidopsis* Col-0 WT seedlings did not display uneven fluorescence distribution after treatment with 2 μM FluorA XI for 15 min. Scale bar indicates 1 mm. Yellow arrow indicates root orientation towards gravity. The fluorescent signal was digitally enhanced to improve visibility.

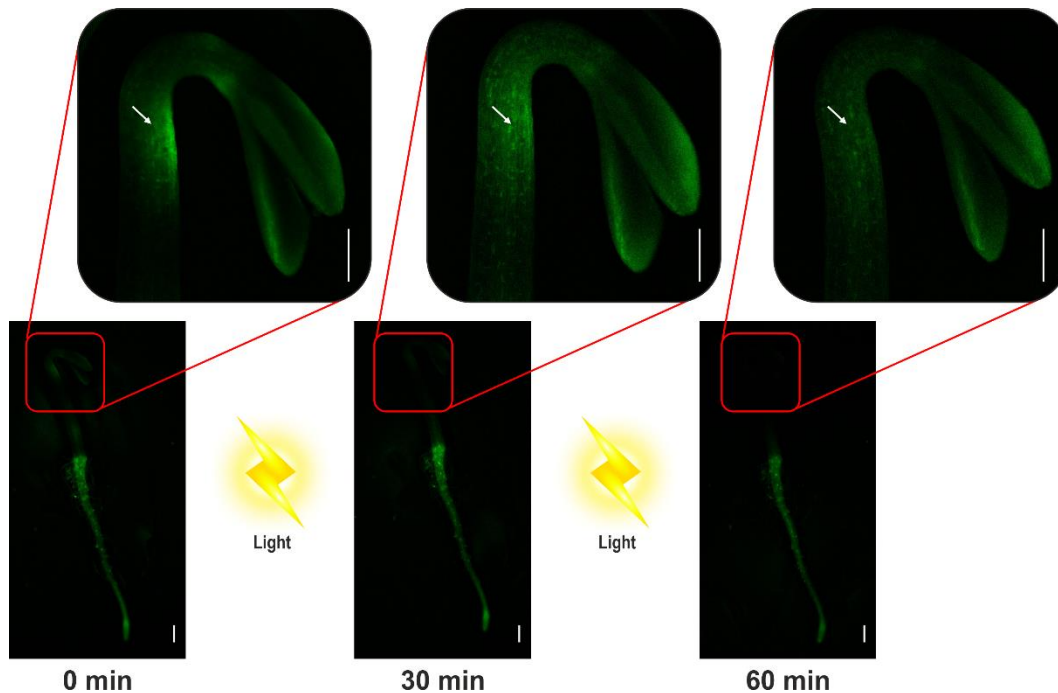


Fig. S5 Tissue-specific distribution of FluorA II in response to light in apical hook. Apical hooks (upper panels) and roots (lower panels) of 3-day-old dark-grown *Arabidopsis thaliana* Col-0 WT seedlings treated in liquid $\frac{1}{2}$ MS media supplemented with 2 μ M FluorA II for 15 min, then transferred onto plates with solid medium containing 2 μ M FluorA II and directly imaged using a vertical macroconfocal (0 min). After that, the plants were transferred to standard light conditions and imaged after a further 30 and 60 min. Persistent fluorescent intensity in roots after the transfer to light demonstrated that FluorA II redistribution in apical hooks is tissue-specific and was not due to light-induced degradation of the compound. Scale bars represent 1 mm. The white arrows indicate the redistribution of FluorA II signal in apical hook after light stimulation.

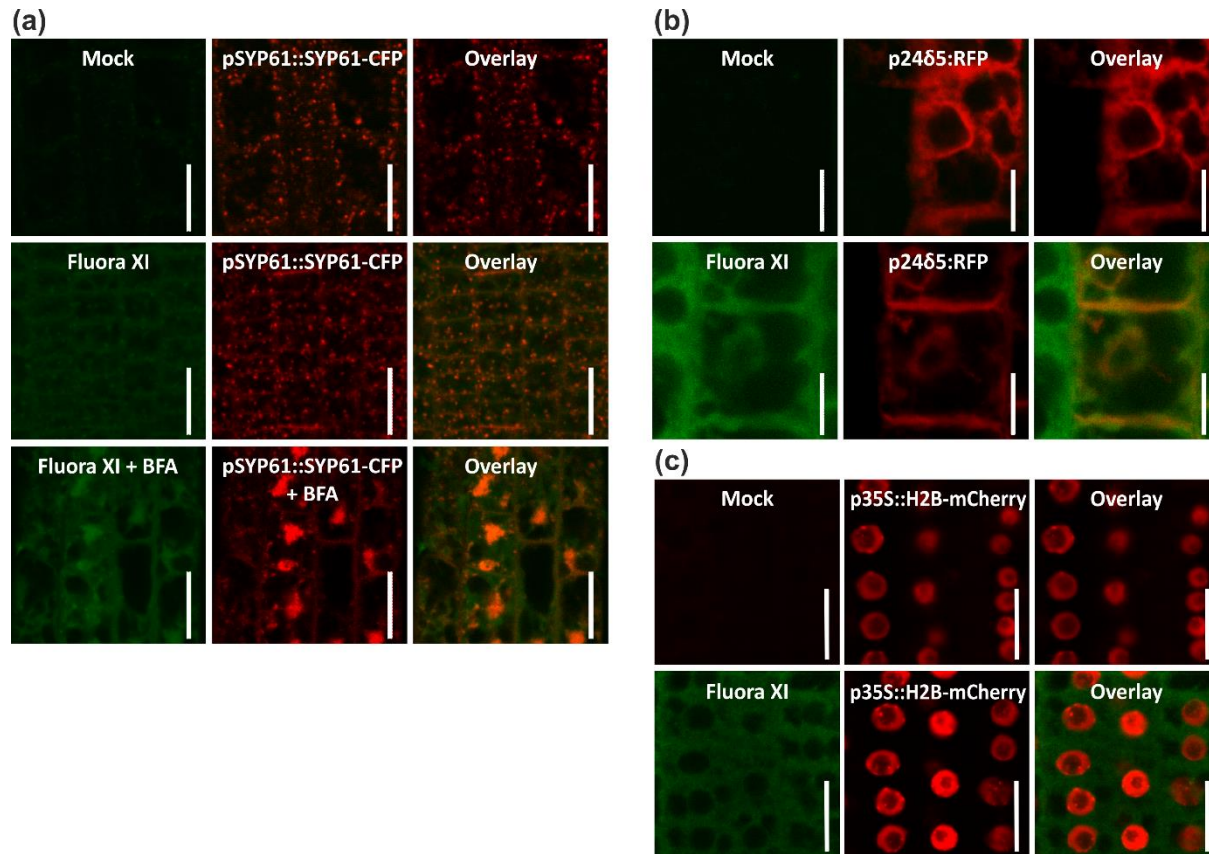


Fig. S6 Subcellular localization of FluorA XI. (a) Five-day old *Arabidopsis* expressing *SYP61::SYP61-CFP* were pre-treated with DMSO or BFA for 3 h before adding 2 μ M FluorA XI or DMSO for 15 minutes. The RFP channels have been digitally enhanced in the same fashion for all panels to improve visualization of endosomes. Scale bar indicates 20 μ m. (b) Five-day-old *Arabidopsis* seedlings expressing *p24δ5::RFP* were treated in liquid medium supplemented with 2 μ M FluorA XI or DMSO for 15 minutes. Scale bar indicates 10 μ m. (c) Five-day-old *Arabidopsis* expressing *p35S::H2B-mCherry* were treated in liquid medium supplemented with 2 μ M FluorA XI or DMSO for 15 minutes. Scale bar indicates 20 μ m. (a-c) The NBD channels have been digitally enhanced in the same fashion for all panels to improve visualization of FluorA XI fluorescence and the co-localization of FluorA XI with particular markers.

Table S1 Quantification of *Arabidopsis* primary root length after 5 days of treatment with FluorA compounds. Effect of FluorA compounds on primary root growth of *Arabidopsis thaliana* evaluated after 5 days of plant growth in the presence of FluorAs at indicated concentrations. Statistical analyses were performed using the Student's t-test to compare to DMSO (values are means \pm SE; n = 10 from 2 independent biological replicates; no asterisks indicate p-value > 0.1; *: p-value < 0.05; ***: p-value < 0.001).

Treatment	[μ M]	Root length [cm]
DMSO	[0]	0.494 \pm 0.019
2,4-D	[1]	0.051 \pm 0.006***
	[10]	0.050 \pm 0.002***
	[50]	0.046 \pm 0.004***
FluorA I	[1]	0.226 \pm 0.059***
	[10]	0.065 \pm 0.008***
	[50]	0.049 \pm 0.006***
FluorA II	[1]	0.095 \pm 0.011***
	[10]	0.054 \pm 0.003***
	[50]	0.098 \pm 0.017***
FluorA III	[1]	0.081 \pm 0.011***
	[10]	0.060 \pm 0.005***
	[50]	0.077 \pm 0.002***
FluorA IV	[1]	0.560 \pm 0.047
	[10]	0.236 \pm 0.082***
	[50]	0.075 \pm 0.011***
FluorA V	[1]	0.486 \pm 0.034
	[10]	0.067 \pm 0.004***
	[50]	0.054 \pm 0.003***
FluorA VI	[1]	0.513 \pm 0.068
	[10]	0.054 \pm 0.005***
	[50]	0.048 \pm 0.005***
FluorA VII	[1]	0.390 \pm 0.027*
	[10]	0.051 \pm 0.005***
	[50]	0.050 \pm 0.008***
FluorA VIII	[1]	0.425 \pm 0.028
	[10]	0.083 \pm 0.006***
	[50]	0.045 \pm 0.005***
FluorA IX	[1]	0.105 \pm 0.010***
	[10]	0.058 \pm 0.003***
	[50]	0.048 \pm 0.003***
FluorA X	[1]	0.566 \pm 0.026
	[10]	0.539 \pm 0.025
	[50]	0.418 \pm 0.042
FluorA XI	[1]	0.552 \pm 0.030
	[10]	0.552 \pm 0.042
	[50]	0.430 \pm 0.026

DMSO – dimethyl sulfoxide;

2,4-D – 2,4-dichlorophenoxyacetic acid

Table S2 Uptake and metabolization of FluorA compounds *in planta* determined by sensitive liquid chromatography–mass spectrometry (LC-MS) detection. Time-course analysis of FluorA compounds and free 2,4-D internal levels in *Arabidopsis thaliana* roots during treatment with 10 μ M FluorAs. Values are means \pm SD (n = 5).

Treatment	time [h]	FluorA [pmol/50 roots]	2,4-D [pmol/50 roots]	Free 2,4-D [%]
FluorA I [10 μ M]	0	166.5 \pm 9.3	0.38 \pm 0.12	0%
	0.5	326.5 \pm 15.2	5.79 \pm 0.66	2%
	1	352.5 \pm 6.7	8.39 \pm 0.28	2%
	2	330.2 \pm 8.6	13.30 \pm 0.01	4%
	3	352.1 \pm 15.7	20.07 \pm 0.53	5%
FluorA II [10 μ M]	0	79.3 \pm 1.5	0.37 \pm 0.04	0%
	0.5	261.1 \pm 2.9	7.81 \pm 0.06	3%
	1	311.2 \pm 2.2	9.46 \pm 0.36	3%
	2	392.2 \pm 4.2	16.32 \pm 0.53	4%
	3	512.0 \pm 10.7	28.66 \pm 0.50	5%

2,4-D – 2,4-dichlorophenoxyacetic acid

Table S3 LC-MS determination of 2,4-D uptake to *Arabidopsis* roots after treatment of *Arabidopsis* seedlings with increasing 2,4-D concentrations. Quantification of internal levels of 2,4-D in roots with respect to external 2,4-D concentrations after 15 min of treatment. Values are means \pm SD (n = 4).

External 2,4-D concentration [nM]	Internal 2,4-D levels [pmol/50 roots]
10	ND
25	0.079 \pm 0.039
50	0.31 \pm 0.09
75	0.46 \pm 0.13
100	0.98 \pm 0.07

2,4-D – 2,4-dichlorophenoxyacetic acid; ND – not detected

Table S4 Biological activity of FluorA compounds estimated by the quantification of Venus fluorescence signal in *p35S::DII-Venus Arabidopsis* seedlings in response to FluorA treatment. 15 min treatments of five-day-old *p35S::DII-Venus Arabidopsis thaliana* seedlings with FluorAs and free 2,4-D providing equivalent amount of internal free 2,4-D result in similar auxin response, measured as degradation in the fluorescence intensity of Venus signal in the root tips. Statistical analyses were performed using the Student's *t*-test to compare to DMSO (values are means \pm SE; *n* = 30 from 3 independent biological replicates; *p*-values: **P*<0.05; ****P* < 0.0005).

Treatment	Fluorescence intensity
DMSO	23.13 \pm 1.27
230 nM 2,4-D	12.88 \pm 0.82***
10 μ M FluorA I	16.52 \pm 2.61*
10 μ M FluorA II	15.95 \pm 2.37*

DMSO – dimethyl sulfoxide; 2,4-D – 2,4-dichlorophenoxyacetic acid

Table S5 Effect of active auxin efflux on FluorA distribution in primary root of *Arabidopsis thaliana*. Fluorescence intensity of FluorA in the root relative to the control samples (Col-0 without NPA). Statistical analyses were performed using the Student's *t*-test to compare to the control samples (values are means \pm SE; *n* = 30 from 3 independent biological replicates; *p*-values: ***P* < 0.001; ****P* < 0.0001).

Treatment	Relative fluorescence intensity
Col-0 + FluorA I [2 μ M]	1.00 \pm 0.10
Col-0 + NPA [10 μ M] + FluorA I [2 μ M]	1.56 \pm 0.19**
Col-0 + FluorA II [2 μ M]	1.00 \pm 0.05
Col-0 + NPA [10 μ M] + FluorA II [2 μ M]	1.63 \pm 0.07***

NPA – *N*-1-naphthylphthalamic acid

Table S6 Effect of active auxin influx on FluorA uptake in primary root of *Arabidopsis thaliana*. Fluorescence intensity of FluorA in the root relative to the control samples (Col-0 without 2-NOA). Statistical analyses were performed using the Student's *t*-test to compare to the control samples (values are means \pm SE; n = 30 from 3 independent biological replicates; p-values: P > 0.1).

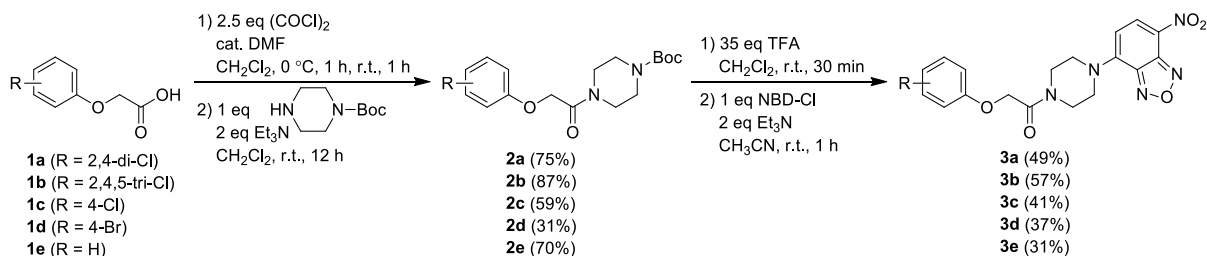
Treatment	Relative fluorescence intensity
Col-0 + FluorA I [2 μ M]	1.00 \pm 0.06
<i>aux1-21/ax3</i> + FluorA I [2 μ M]	0.98 \pm 0.10
Col-0 + 2-NOA [10 μ M] + FluorA I [2 μ M]	1.13 \pm 0.13
Col-0 + FluorA II [2 μ M]	1.00 \pm 0.04
<i>aux1-21/ax3</i> + FluorA II [2 μ M]	0.97 \pm 0.14
Col-0 + 2-NOA [10 μ M] + FluorA II [2 μ M]	1.03 \pm 0.04
2-NOA – 2-naphthoxyacetic acid	

Methods S1 Synthesis of FluorA compounds.

1.1. General methods. Reagents and solvents were purchased from common commercial suppliers and used without further purification. Dichloromethane and acetonitrile were distilled from calcium hydride, while dimethylformamide was dried over molecular sieves before use. The conversion of starting materials was monitored by thin layer chromatography (TLC) on aluminium plates coated with silica gel 60 F254 (Merck, USA) and the components were visualized by UV light (254 and 365 nm) and staining solutions (ninhydrin and potassium permanganate). The purification of the reaction mixtures was performed by column chromatography on silica gel (40-63 micron Davisil LC60A, Grace Davison, UK). ^1H (500 MHz) and ^{13}C (126 MHz) NMR spectra were recorded at room temperature (Jeol ECA-500 NMR, Japan) in deuterated solvents (CDCl_3 or $\text{DMSO-}d_6$) as indicated for each compound. Peak assignments were elucidated *via* APT and HMQC techniques when necessary. The chromatographic purity and mass spectra of the prepared compounds were analyzed using high performance liquid chromatography–photodiode array–mass spectrometry (HPLC–PDA–MS) method. Compounds (10 μl of 3.10^{-5} M in 0.01% DMSO) were injected onto a reverse-phased column (Symmetry C18, 5 μm , 150 mm \times 2.1 mm; Waters, Milford, MA, USA) equilibrated at 25 $^\circ\text{C}$ with solvent (A), which consisted of 15 mM ammonium formate adjusted to pH 4.0 and solvent (B), which consisted of methanol. At a flow-rate of 200 $\mu\text{l}/\text{min}$, the following binary gradient was used: 0 min, 10% B; 0-24 min, linear gradient to 90% B; 25-34 min, isocratic elution of 90% B; 35-45 min, linear gradient to 10% B using an Alliance 2695 Separations Module (Waters, Milford, MA, USA). The effluent was then introduced to a 2996 PDA detector (Waters, Milford, MA, USA) (scanning range 210-700 nm with 1.2 nm resolution) and a tandem mass analyser Q-ToF micro Mass Spectrometer (Waters, Manchester, UK) with an electrospray source (source temperature 120 $^\circ\text{C}$, desolvation temperature 300 $^\circ\text{C}$, capillary voltage 3 kV). Nitrogen was used as well as cone gas (50 l/h) and desolvation gas (500 l/h). Data acquisition was performed in the full scan mode (50-1000 Da), with scan time of 0.5 s and cone voltage 20 V. Analyses were performed in positive (ESI+) and negative (ESI-) mode and molecular ions were recorded in $[\text{M}+\text{H}]^+$ and $[\text{M}-\text{H}]^-$ or $[\text{M}+\text{HCOOH}-\text{H}]^-$, forms, respectively.

1.2. General procedure for the synthesis of 2a-e and 3a-e (Scheme I). Synthesis of *tert*-butyl 4-(2-(2,4-dichlorophenoxy)acetyl)piperazine-1-carboxylate (**2a**) is representative. 2,4-D (**1a**; 441 mg, 2 mmol) was dissolved in anhydrous dichloromethane (20 ml) and cooled down to 0 $^\circ\text{C}$. Subsequently, dimethylformamide (30 μl) and oxalyl chloride (0.43 ml, 5 mmol) were added drop-wise with vigorous stirring and the resulting reaction mixture was stirred at 0 $^\circ\text{C}$ for 1 hour and then at room temperature for the next 1 hour. Evaporation of the solvent under reduced pressure in a cold water bath afforded intermediate 2-(2,4-dichlorophenoxy)acetyl chloride in a quantitative yield, which was used in the next step without further purification or characterization. The residual crude 2-(2,4-dichlorophenoxy)acetyl chloride was dissolved in anhydrous dichloromethane (10 ml) and cooled down to 0 $^\circ\text{C}$. Subsequently, triethylamine (0.56 ml, 4 mmol) was added drop-wise, followed by *tert*-butyl piperazine-1-carboxylate (1-Boc-piperazine) (372 mg, 2 mmol), allowed to warm up to room temperature and the resulting reaction mixture was stirred for 12 h. Upon completion, the reaction mixture was cooled down to 0 $^\circ\text{C}$, quenched with water (10 ml) and extracted with ethyl acetate (3 \times 20 ml). Combined

organic fractions were washed with water (10 ml) and brine (10 ml), dried over anhydrous sodium sulphate, filtered and concentrated under reduced pressure. Purification of the residue by flash chromatography on silica gel afforded compound **2a**. Synthesis of *tert*-butyl 2-(2,4-dichlorophenoxy)-1-(4-(7-nitrobenzo[*c*][1,2,5]oxadiazol-4-yl)piperazin-1-yl)ethanone (**3a, FluorA II**) is representative. Compound **2a** (129 mg, 0.33 mmol) was dissolved in anhydrous dichloromethane (4 ml) and cooled down to 0 °C. Subsequently, trifluoroacetic acid (0.825 ml) was added drop-wise with vigorous stirring, the reaction mixture was allowed to warm up to room temperature and the resulting reaction mixture was stirred for 30 minutes at room temperature. Subsequently, the reaction mixture was cooled down to 0 °C, quenched with saturated aqueous sodium bicarbonate solution (to pH = 7) and extracted with ethyl acetate (3 × 20 ml). Combined organic fractions were washed with water (10 ml) and brine (10 ml), dried over anhydrous sodium sulphate, filtered and concentrated under reduced pressure to afford intermediate 2-(2,4-dichlorophenoxy)-1-(piperazin-1-yl)ethanone in a quantitative yield, which was used in the next step without further purification or characterization. The residual 2-(2,4-dichlorophenoxy)-1-(piperazin-1-yl)ethanone was dissolved in acetonitrile (7 ml), to which triethylamine (92 μl, 0.66 mmol) was added drop-wise, followed by 4-chloro-7-nitrobenzofurazan, NBD-Cl (66 mg, 0.33 mmol) at 0 °C. The reaction mixture was stirred at room temperature for 1 hour. The reaction mixture was quenched with saturated ammonium chloride solution (10 ml) and extracted with ethyl acetate (3 × 20 ml). Combined organic fractions were washed with water (10 ml) and brine (10 ml), dried over anhydrous sodium sulphate, filtered and concentrated under reduced pressure. Purification of the residue by flash chromatography on silica gel afforded compound **3a**.



Scheme I

tert-Butyl 4-(2-(2,4-dichlorophenoxy)acetyl)piperazine-1-carboxylate (**2a**): white solid, $R_f = 0,29$ (petroleum ether/ethyl acetate 3/2), yield 75%. ¹H NMR (500 MHz, CDCl₃): δ 7.38 (d, $J = 2.45$ Hz, 1H), 7.17 (d, $J = 8.86$, 2.45 Hz, 1H), 6.94 (d, $J = 8.86$ Hz, 1H), 4.76 (s, 2H), 3.62 – 3.53 (m, 4H), 3.46 – 3.35 (m, 4H), 1.45 (s, 9H). ¹³C NMR (126 MHz, CDCl₃): δ 165.8, 154.5, 152.0, 130.4, 127.9, 127.1, 123.6, 114.3, 80.6, 68.9, 45.6, 42.2, 28.4. MS (ESI⁺): m/z (%) = 388.7357 ([M+H]⁺, 25). HPLC–UV purity: 99.06%.

2-(2,4-Dichlorophenoxy)-1-(4-(7-nitrobenzo[*c*][1,2,5]oxadiazol-4-yl)piperazin-1-yl)ethan-1-one (**3a, FluorA II**): orange solid, $R_f = 0.41$ (CH₂Cl₂/acetone 20/1), yield 49%. ¹H NMR (500 MHz, DMSO-*d*₆): δ 8.49 (d, $J = 9.2$ Hz, 1H), 7.54 (d, $J = 2.8$ Hz, 1H), 7.30 (dd, $J = 8.9$, 2.8 Hz, 1H), 7.06 (d, $J = 8.9$ Hz, 1H), 6.60 (d, $J = 9.2$ Hz, 1H), 5.05 (s, 2H), 4.29 – 4.10 (m, 4H), 3.80 – 3.67 (m, 4H). ¹³C NMR (126 MHz, DMSO-*d*₆): δ 166.2, 153.2, 146.0, 145.4, 145.3, 136.9, 129.8, 128.3, 125.1, 122.7, 121.8, 115.8, 103.8, 66.9, 49.3, 49.0, 43.3, 41.1. MS (ESI⁻): m/z (%) = 496.2106 ([M+HCOOH-H]⁻, 100). HPLC–UV purity: 99.19%.

tert-Butyl 4-(2-(2,4,5-trichlorophenoxy)acetyl)piperazine-1-carboxylate (**2b**): white solid, $R_f = 0.29$ (petroleum ether/ethyl acetate 2/1), yield 87%. $^1\text{H NMR}$ (500 MHz, CDCl_3): δ 7.46 (s, 1H), 7.08 (s, 1H), 4.75 (s, 2H), 3.61 – 3.52 (m, 4H), 3.49 – 3.38 (m, 4H), 1.46 (s, 9H). $^{13}\text{C NMR}$ (126 MHz, CDCl_3): δ 165.2, 154.5, 152.3, 131.6, 131.3, 125.6, 122.1, 115.2, 80.6, 68.8, 45.5, 42.2, 28.4. MS (ESI+): m/z (%) = 422.8232 ($[\text{M}+\text{H}]^+$, 20). HPLC–UV purity: 99.74%. 1-(4-(7-Nitrobenzo[*c*][1,2,5]oxadiazol-4-yl)piperazin-1-yl)-2-(2,4,5-trichlorophenoxy)ethan-1-one (**3b**, **FluorA VII**): orange solid, $R_f = 0.47$ (CH_2Cl_2 /acetone 20/1), yield 57%. $^1\text{H NMR}$ (500 MHz, $\text{DMSO-}d_6$): δ 8.48 (d, $J = 9.1$ Hz, 1H), 7.77 (s, 1H), 7.42 (s, 1H), 6.60 (d, $J = 9.2$ Hz, 1H), 5.11 (s, 2H), 4.28 – 4.11 (m, 4H), 3.76 – 3.69 (m, 4H). $^{13}\text{C NMR}$ (126 MHz, $\text{DMSO-}d_6$): δ 165.9, 153.7, 146.0, 145.4, 145.3, 136.9, 131.0, 130.7, 123.4, 121.8, 121.6, 116.2, 103.8, 67.1, 49.2, 49.0, 43.2, 41.1. MS (ESI-): m/z (%) = 530.1920 ($[\text{M}+\text{HCOOH-}\text{H}]^-$, 100). HPLC–UV purity: 98.42%.

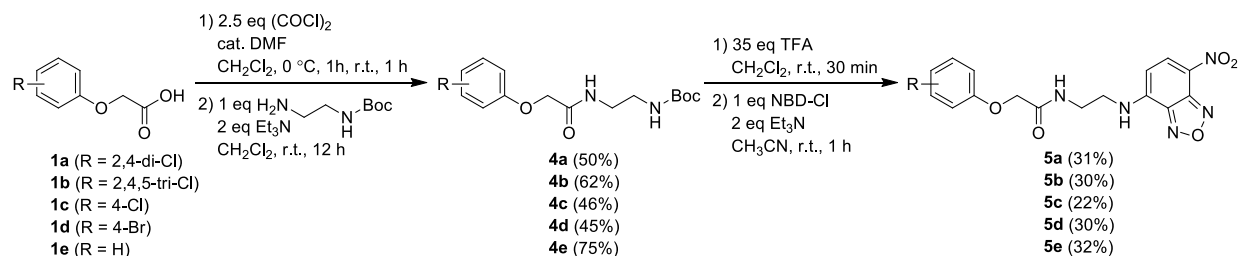
tert-Butyl 4-(2-(4-chlorophenoxy)acetyl)piperazine-1-carboxylate (**2c**): white solid, $R_f = 0.29$ (petroleum ether/ethyl acetate 3/2), yield 59%. $^1\text{H NMR}$ (500 MHz, CDCl_3): δ 7.22 (d, $J = 9.0$ Hz, 1H), 6.86 (d, $J = 9.0$ Hz, 1H), 4.66 (s, 2H), 3.59 – 3.49 (m, 4H), 3.43 – 3.34 (m, 4H), 1.44 (s, 9H). $^{13}\text{C NMR}$ (126 MHz, CDCl_3): δ 166.4, 156.4, 154.5, 129.7, 126.8, 116.0, 80.5, 68.0, 45.4, 42.1, 28.4. MS (ESI+): m/z (%) = 354.9385 ($[\text{M}+\text{H}]^+$, 20). HPLC–UV purity: 98.94%. 2-(4-Chlorophenoxy)-1-(4-(7-nitrobenzo[*c*][1,2,5]oxadiazol-4-yl)piperazin-1-yl)ethan-1-one (**3c**, **FluorA IX**): orange solid, $R_f = 0.32$ (CH_2Cl_2 /acetone 20/1), yield 41%. $^1\text{H NMR}$ (500 MHz, $\text{DMSO-}d_6$): δ 8.48 (d, $J = 9.1$ Hz, 1H), 7.28 (d, $J = 9.0$ Hz, 2H), 6.93 (d, $J = 9.1$ Hz, 2H), 6.59 (d, $J = 9.2$ Hz, 1H), 4.88 (s, 2H), 4.26 – 4.09 (m, 4H), 3.78 – 3.68 (m, 4H). $^{13}\text{C NMR}$ (126 MHz, $\text{DMSO-}d_6$): δ 166.7, 157.5, 146.0, 145.4, 145.3, 136.9, 129.6, 125.1, 121.8, 117.0, 103.8, 66.4, 49.3, 49.0, 43.3, 41.1. MS (ESI+): m/z (%) = 462.3372 ($[\text{M}+\text{HCOOH-}\text{H}]^-$, 100). HPLC–UV purity: 98.97%.

tert-Butyl 4-(2-(4-bromophenoxy)acetyl)piperazine-1-carboxylate (**2d**): white solid, $R_f = 0.23$ (petroleum ether/ethyl acetate 3/2), yield 31%. $^1\text{H NMR}$ (300 MHz, CDCl_3): δ 7.38 (d, $J = 9.1$ Hz, 2H), 6.82 (d, $J = 9.1$ Hz, 2H), 4.67 (s, 2H), 3.63 – 3.48 (m, 4H), 3.46 – 3.34 (m, 4H), 1.45 (s, 9H). $^{13}\text{C NMR}$ (126 MHz, CDCl_3): δ 166.4, 156.9, 154.5, 132.6, 116.5, 114.2, 80.6, 68.0, 45.4, 42.1, 28.4. MS (ESI+): m/z (%) = 398.8239 ($[\text{M}+\text{H}]^+$, 20). HPLC–UV purity: 95.64%. 2-(4-Bromophenoxy)-1-(4-(7-nitrobenzo[*c*][1,2,5]oxadiazol-4-yl)piperazin-1-yl)ethan-1-one (**3d**, **FluorA V**): orange solid, $R_f = 0.32$ (CH_2Cl_2 /acetone 20/1), yield 37%. $^1\text{H NMR}$ (500 MHz, $\text{DMSO-}d_6$): δ 8.46 (d, $J = 9.1$ Hz, 1H), 7.39 (d, $J = 9.1$ Hz, 2H), 6.88 (d, $J = 9.1$ Hz, 2H), 6.56 (d, $J = 9.2$ Hz, 1H), 4.88 (s, 2H), 4.25 – 4.08 (m, 4H), 3.79 – 3.68 (m, 4H). $^{13}\text{C NMR}$ (126 MHz, $\text{DMSO-}d_6$): δ 166.7, 157.9, 146.0, 145.31, 145.27, 136.9, 132.5, 121.7, 117.5, 112.8, 103.8, 66.3, 49.3, 49.0, 43.2, 41.0. MS (ESI-): m/z (%) = 506.1949 ($[\text{M}+\text{HCOOH-}\text{H}]^-$, 100). HPLC–UV purity: >99.9%.

tert-Butyl 4-(2-phenoxyacetyl)piperazine-1-carboxylate (**2e**): white solid, $R_f = 0.29$ (petroleum ether/ethyl acetate 3/2), yield 70%. $^1\text{H NMR}$ (500 MHz, CDCl_3): δ 7.32–7.27 (m, 2H), 7.00 (t, $J = 7.4$ Hz, 1H), 6.94 (d, $J = 8.7$ Hz, 2H), 4.70 (s, 2H), 3.61 – 3.54 (m, 4H), 3.45 – 3.36 (m, 4H), 1.45 (s, 9H). $^{13}\text{C NMR}$ (126 MHz, CDCl_3): δ 166.8, 157.7, 154.6, 129.8, 121.9, 114.6, 80.5, 67.9, 45.5, 42.1, 28.5. MS (ESI+): m/z (%) = 321.0084 ($[\text{M}+\text{H}]^+$, 30). HPLC–UV purity: 97.48%.

1-(4-(7-Nitrobenzo[*c*][1,2,5]oxadiazol-4-yl)piperazin-1-yl)-2-phenoxyethan-1-one (**3e**, **Fluora XI**): orange solid, $R_f = 0.29$ (CH_2Cl_2 /acetone 20/1), yield 31%. $^1\text{H NMR}$ (500 MHz, $\text{DMSO-}d_6$): δ 8.49 (d, $J = 9.1$ Hz, 1H), 7.26 – 7.22 (m, 2H), 6.93 – 6.86 (m, 3H), 6.60 (d, $J = 9.2$ Hz, 1H), 4.85 (s, 1H), 4.27 – 4.11 (m, 4H), 3.81 – 3.68 (m, 4H). $^{13}\text{C NMR}$ (126 MHz, $\text{DMSO-}d_6$): δ 167.0, 158.5, 146.0, 145.4, 145.3, 136.9, 129.9, 121.8, 121.4, 115.1, 103.8, 66.2, 49.4, 49.0, 43.4, 41.1. MS (ESI+): m/z (%) = 428.3476 ($[\text{M}+\text{HCOOH-}\text{H}]^-$, 100). HPLC–UV purity: 98.13%.

1.3. General procedure for the synthesis of 4a-e and 5a-e (Scheme II). Synthesis of *tert*-butyl (2-(2-(2,4-dichlorophenoxy)acetamido)ethyl)carbamate (**4a**) is representative. 2,4-D (**1a**; 221 mg, 1 mmol) was dissolved in anhydrous dichloromethane (10 ml) and cooled down to 0 °C. Subsequently, dimethylformamide (15 μ l) and oxalyl chloride (0.215 ml, 2.5 mmol) were added drop-wise with vigorous stirring and the resulting reaction mixture was stirred at 0 °C for 1 hour and then at room temperature for the next 1 hour. Evaporation of the solvent under reduced pressure in a cold water bath afforded the intermediate 2-(2,4-dichlorophenoxy)acetyl chloride in a quantitative yield, which was used in the next step without further purification or characterization. The residual crude 2-(2,4-dichlorophenoxy)acetyl chloride was dissolved in anhydrous dichloromethane (10 ml) and cooled down to 0 °C. Subsequently, triethylamine (278 μ l, 2 mmol) was added drop-wise, followed by *tert*-butyl *N*-(2-aminoethyl)carbamate (*N*-Boc-ethylenediamine) (160 mg, 1 mmol), allowed to warm up to room temperature and the resulting reaction mixture was stirred for 12 h. Upon completion, the reaction mixture was cooled down to 0 °C, quenched with water (5 ml) and extracted with ethyl acetate (3 \times 15 ml). Combined organic fractions were washed with water (5 ml) and brine (5 ml), dried over anhydrous sodium sulphate, filtered and concentrated under reduced pressure. Purification of the residue by flash chromatography on silica gel afforded compound **4a**. Synthesis of 2-(2,4-dichlorophenoxy)-*N*-(2-((7-nitrobenzo[*c*][1,2,5]oxadiazol-4-yl)amino)ethyl) acetamide (**5a**, **FluorA I**) is representative. Compound **4a** (140 mg, 0.386 mmol) was dissolved in anhydrous dichloromethane (4 ml) and cooled down to 0 °C. Subsequently, trifluoroacetic acid (1 ml) was added drop-wise with vigorous stirring, the reaction mixture was allowed to warm up to room temperature and the resulting reaction mixture was stirred for 30 minutes at room temperature. Subsequently, the reaction mixture was cooled down to 0 °C, quenched with saturated aqueous sodium bicarbonate solution (to pH 7) and extracted with ethyl acetate (3 \times 20 ml). Combined organic fractions were washed with water (10 ml) and brine (10 ml), dried over anhydrous sodium sulphate, filtered and concentrated under reduced pressure to afford the intermediate *N*-(2-aminoethyl)-2-(2,4-dichlorophenoxy)acetamide in a quantitative yield, which was used in the next step without further purification or characterization. The residual *N*-(2-aminoethyl)-2-(2,4-dichlorophenoxy)acetamide was dissolved in acetonitrile (15 ml), to which triethylamine (107 μ l, 0.771 mmol) was added drop-wise, followed by 4-chloro-7-nitrobenzofurazan, NBD-Cl (77 mg, 0.386 mmol) at 0 °C. The reaction mixture was stirred at room temperature for 1 hour. The reaction mixture was quenched with saturated ammonium chloride solution (10 ml) and extracted with ethyl acetate (3 \times 20 ml). Combined organic fractions were washed with water (10 ml) and brine (10 ml), dried over anhydrous sodium sulphate, filtered and concentrated under reduced pressure. Purification of the residue by flash chromatography on silica gel afforded compound **5a**.



Scheme II

tert-Butyl (2-(2-(2,4-dichlorophenoxy)acetamido)ethyl)carbamate (**4a**): white solid, $R_f = 0.14$ (petroleum ether/ethyl acetate 3/2), yield 50%. $^1\text{H NMR}$ (500 MHz, CDCl_3): δ 7.40 (d, $J = 2.5$ Hz, 1H), 7.21 (dd, $J = 8.9, 2.5$ Hz, 1H), 7.17-7.10 (br s, 1H), 6.82 (d, $J = 8.9$ Hz, 1H), 4.85-4.78 (br s, 1H), 4.51 (s, 2H), 3.51-3.46 (m, 2H), 3.34-3.27 (m, 2H), 1.41 (s, 9H). $^{13}\text{C NMR}$ (126 MHz, $\text{DMSO-}d_6$): δ 167.5, 156.2, 153.0, 129.8, 128.6, 125.6, 123.0, 115.9, 78.2, 68.3, 40.0, 39.1, 28.7. MS (ESI+): m/z (%) = 362.7133 ($[\text{M}+\text{H}]^+$, 20). HPLC–UV purity: 96.77%.

2-(2,4-Dichlorophenoxy)-*N*-(2-((7-nitrobenzo[*c*][1,2,5]oxadiazol-4-yl)amino)ethyl)acetamide (**5a, FluorA I**): orange solid, $R_f = 0.26$ (CH_2Cl_2 /acetone 20/1), yield 31%. $^1\text{H NMR}$ (500 MHz, $\text{DMSO-}d_6$): δ 9.40 – 9.33 (br s, 1H), 8.48 (d, $J = 8.9$ Hz, 1H), 8.18 – 8.12 (m, 1H), 7.51 (d, $J = 2.5$ Hz, 1H), 7.21 (dd, $J = 8.9, 2.5$ Hz, 1H), 6.96 (d, $J = 8.9$ Hz, 1H), 6.41 (d, $J = 8.9$ Hz, 1H), 4.58 (s, 2H), 3.58 – 3.51 (m, 2H), 3.47 – 3.42 (m, 2H). $^{13}\text{C NMR}$ (126 MHz, $\text{DMSO-}d_6$): δ 168.3, 152.8, 145.9, 144.9, 144.5, 138.5, 129.8, 128.4, 125.7, 123.0, 121.4, 115.8, 99.7, 68.4, 43.4, 37.6. MS (ESI-): m/z (%) = 424.1541 ($[\text{M}-\text{H}]^-$, 100). HPLC–UV purity: 99.30%.

tert-Butyl (2-(2-(2,4,5-trichlorophenoxy)acetamido)ethyl)carbamate (**4b**): white solid, $R_f = 0.23$ (petroleum ether/ethyl acetate 3/2), yield 62%. $^1\text{H NMR}$ (500 MHz, CDCl_3): δ 7.49 (s, 1H), 7.20 – 7.10 (br s, 1H), 6.99 (s, 1H), 4.90 – 4.80 (br s, 1H), 4.50 (s, 2H), 3.52 – 3.45 (m, 2H), 3.35 – 3.25 (m, 2H), 1.41 (s, 9H). $^{13}\text{C NMR}$ (126 MHz, CDCl_3): δ 167.3, 156.5, 151.9, 131.8, 131.3, 126.1, 122.3, 115.6, 79.9, 68.5, 40.3, 39.9, 28.4. MS (ESI+): m/z (%) = 396.8232 ($[\text{M}+\text{H}]^+$, 20). HPLC–UV purity: 97.97%.

N-(2-((7-Nitrobenzo[*c*][1,2,5]oxadiazol-4-yl)amino)ethyl)-2-(2,4,5-trichlorophenoxy)acetamide (**5b, FluorA VI**): orange solid, $R_f = 0.32$ (CH_2Cl_2 /acetone 20/1), yield 30%. $^1\text{H NMR}$ (500 MHz, $\text{DMSO-}d_6$): δ 9.37 – 9.30 (br s, 1H), 8.46 (d, $J = 8.9$ Hz, 1H), 8.18 – 8.13 (m, 1H), 7.74 (s, 1H), 7.24 (s, 1H), 6.40 (d, $J = 8.9$ Hz, 1H), 4.65 (s, 2H), 3.57 – 3.43 (m, 4H). $^{13}\text{C NMR}$ (126 MHz, $\text{DMSO-}d_6$): δ 167.9, 153.3, 145.9, 144.9, 144.5, 138.4, 131.1, 130.8, 123.9, 121.9, 121.4, 116.3, 99.7, 68.6, 43.5, 37.7. MS (ESI-): m/z (%) = 458.1182 ($[\text{M}-\text{H}]^+$, 100). HPLC–UV purity: 99.89%.

tert-Butyl (2-(2-(4-chlorophenoxy)acetamido)ethyl)carbamate (**4c**): white solid, $R_f = 0.29$ (petroleum ether/ethyl acetate 1/1), yield 46%. $^1\text{H NMR}$ (500 MHz, CDCl_3): δ 7.27 (d, $J = 9.0$ Hz, 2H), 7.25 – 7.17 (br s, 1H), 6.87 (d, $J = 9.0$ Hz, 2H), 4.92 – 4.70 (br s, 1H), 4.45 (s, 2H), 3.47 – 3.42 (m, 2H), 3.35 – 3.27 (m, 2H), 1.41 (s, 9H). $^{13}\text{C NMR}$ (126 MHz, CDCl_3): δ 168.6, 156.8, 155.9, 129.7, 127.1, 116.1, 80.0, 67.5, 40.5, 40.2, 28.4. MS (ESI+): m/z (%) = 328.9509 ($[\text{M}+\text{H}]^+$, 20). HPLC–UV purity: 96.55%.

2-(4-Chlorophenoxy)-*N*-(2-((7-nitrobenzo[*c*][1,2,5]oxadiazol-4-yl)amino)ethyl)acetamide (**5c, FluorA VIII**): orange solid, $R_f = 0.21$ (CH_2Cl_2 /acetone 20/1), yield 22%. $^1\text{H NMR}$ (500 MHz, $\text{DMSO-}d_6$): δ 9.51 – 9.29 (br s, 1H), 8.57 – 8.39 (m, 1H), 8.38 – 8.21 (br s, 1H), 7.35 – 7.15 (m, 2H), 7.01 – 6.81 (m, 2H), 6.48 – 6.36 (m, 1H), 4.54 (m, 2H), 3.67 – 3.39 (m, 4H). $^{13}\text{C NMR}$ (126 MHz, CDCl_3): δ 168.6, 156.9, 145.9, 144.9, 144.6, 138.5, 129.7, 125.5, 121.5, 117.0, 99.7, 67.8, 43.4, 37.5. MS (ESI+): m/z (%) = 390.1696 ($[\text{M}-\text{H}]^-$, 100). HPLC–UV purity: 96.61%.

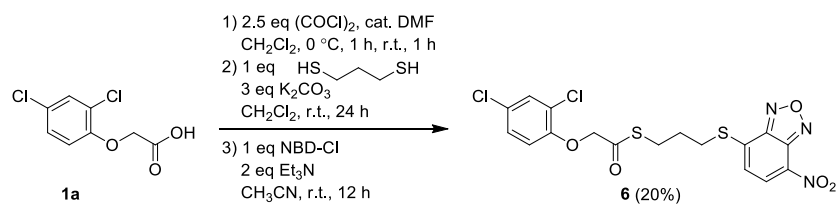
tert-Butyl (2-(2-(4-bromophenoxy)acetamido)ethyl)carbamate (**4d**): white solid, $R_f = 0.29$ (petroleum ether/ethyl acetate 1/1), yield 45%. $^1\text{H NMR}$ (500 MHz, CDCl_3): δ 7.40 (d, $J = 8.86$ Hz, 2H), 7.25 – 7.18 (br s, 1H), 6.82 (d, $J = 9.17$ Hz, 2H), 4.87 – 4.77 (br s, 1H), 4.44 (s, 2H), 3.47 – 3.41 (m, 2H), 3.35 – 3.27 (m, 2H), 1.41 (s, 9H). $^{13}\text{C NMR}$ (126 MHz, CDCl_3): δ 168.5, 156.9, 156.4, 132.7, 116.5, 114.5, 80.0, 67.5, 40.5, 40.2, 28.4. MS (ESI+): m/z (%) = 372.7887 ($[\text{M}+\text{H}]^+$, 20). HPLC–UV purity: <99.9%. 2-(4-Bromophenoxy)-*N*-(2-((7-nitrobenzo[*c*][1,2,5]oxadiazol-4-

yl)amino)ethyl)acetamide (**5d, FluorA IV**): orange solid, $R_f = 0.24$ ($\text{CH}_2\text{Cl}_2/\text{acetone}$ 20/1), yield 30%. ^1H NMR (500 MHz, $\text{DMSO}-d_6$): δ 9.39 – 9.32 (br s, 1H), 8.46 (d, $J = 8.9$ Hz, 1H), 8.31 – 8.26 (m, 1H), 7.35 (d, $J = 8.9$ Hz, 2H), 6.84 (d, $J = 9.2$ Hz, 2H), 6.40 (d, $J = 9.2$ Hz, 1H), 4.43 (s, 2H), 3.55 – 3.39 (m, 4H). ^{13}C NMR (126 MHz, $\text{DMSO}-d_6$): δ 168.6, 157.4, 145.9, 145.0, 144.6, 138.5, 132.6, 121.5, 117.5, 113.2, 99.7, 67.7, 43.4, 37.5. MS (ESI+): m/z (%) = 434.1277 ($[\text{M}-\text{H}]^-$, 100). HPLC–UV purity: 96.21%.

tert-Butyl (2-(2-phenoxyacetamido)ethyl)carbamate (**4e**): white solid, $R_f = 0.11$ (petroleum ether/ethyl acetate 3/2), yield 75%. ^1H NMR (500 MHz, CDCl_3): δ 7.31 (t, $J = 7.7$ Hz, 2H), 7.21 – 7.10 (br s, 1H), 7.02 (t, $J = 7.4$ Hz, 1H), 6.93 (d, $J = 7.8$ Hz, 2H), 4.90 – 4.72 (br s, 1H), 4.48 (s, 2H), 3.48 – 3.42 (m, 2H), 3.34 – 3.26 (m, 2H), 1.42 (s, 9H). ^{13}C NMR (126 MHz, CDCl_3): δ 169.1, 157.3, 156.7, 129.9, 122.2, 114.7, 79.9, 67.2, 40.3, 40.1, 28.4. MS (ESI+): m/z (%) = 295.0136 ($[\text{M}+\text{H}]^+$, 30). HPLC–UV purity: 92.92%.

N-(2-((7-Nitrobenzo[*c*][1,2,5]oxadiazol-4-yl)amino)ethyl)-2-phenoxyacetamide (**5e, FluorA X**): orange solid, $R_f = 0.24$ ($\text{CH}_2\text{Cl}_2/\text{acetone}$ 20/1), yield 32%. ^1H NMR (500 MHz, $\text{DMSO}-d_6$): δ 9.44 – 9.35 (br s, 1H), 8.46 (d, $J = 8.9$ Hz, 1H), 8.32 – 8.26 (m, 1H), 7.20 (t, $J = 7.9$ Hz, 2H), 6.90 – 6.85 (m, 3H), 6.41 (d, $J = 9.2$ Hz, 1H), 4.43 (s, 2H), 3.58 – 3.41 (m, 4H). ^{13}C NMR (126 MHz, $\text{DMSO}-d_6$): δ 168.9, 158.1, 145.9, 145.0, 144.6, 138.4, 130.0, 121.7, 121.4, 115.2, 99.7, 67.5, 43.4, 37.5. MS (ESI+): m/z (%) = 356.2428 ($[\text{M}-\text{H}]^-$, 100). HPLC–UV purity: 99.39%.

1.4. General procedure for the synthesis of 6 (Scheme III). 2,4-D (**1a**; 220 mg, 1 mmol) was dissolved in anhydrous dichloromethane (10 ml) and cooled down to 0 °C. Subsequently, dimethylformamide (15 μl) and oxalyl chloride (0.215 ml, 2.5 mmol) were added drop-wise with vigorous stirring and the resulting reaction mixture was stirred at 0 °C for 1 hour and then at room temperature for the next 1 hour. Evaporation of the solvent under reduced pressure in a cold water bath afforded intermediate 2-(2,4-dichlorophenoxy)acetyl chloride in a quantitative yield, which was used in the next step without further purification or characterization. The residual crude 2-(2,4-dichlorophenoxy)acetyl chloride was dissolved in anhydrous dichloromethane (10 ml) and cooled down to 0 °C. Subsequently, potassium carbonate (414 mg, 3 mmol) and propane-1,3-dithiol (0.1 ml, 1 mmol) were added with vigorous stirring and the resulting reaction mixture was stirred at room temperature for 24 h. Upon completion, the reaction mixture was filtered to remove excess potassium carbonate and the filtrate was evaporated. The resulting intermediate S-(3-mercaptopropyl) 2-(2,4-dichlorophenoxy)ethanethioate was dissolved in acetonitrile (10 ml), to which triethylamine (278 μl , 2mmol) was added drop-wise, followed by 4-chloro-7-nitrobenzofurazan, NBD-Cl (200 mg, 1 mmol) at 0 °C. The reaction mixture was stirred at room temperature for 12 h. Upon completion, the reaction mixture was quenched with water (5 ml) and extracted with ethyl acetate (3 \times 20 ml). Combined organic fractions were washed with water (5 ml) and brine (5 ml), dried over anhydrous sodium sulphate, filtered and concentrated under reduced pressure. Purification of the residue by flash chromatography on silica gel afforded S-(3-((7-nitrobenzo[*c*][1,2,5]oxadiazol-4-yl)thio)propyl) 2-(2,4-dichlorophenoxy) ethanethioate (**6, FluorA III**).

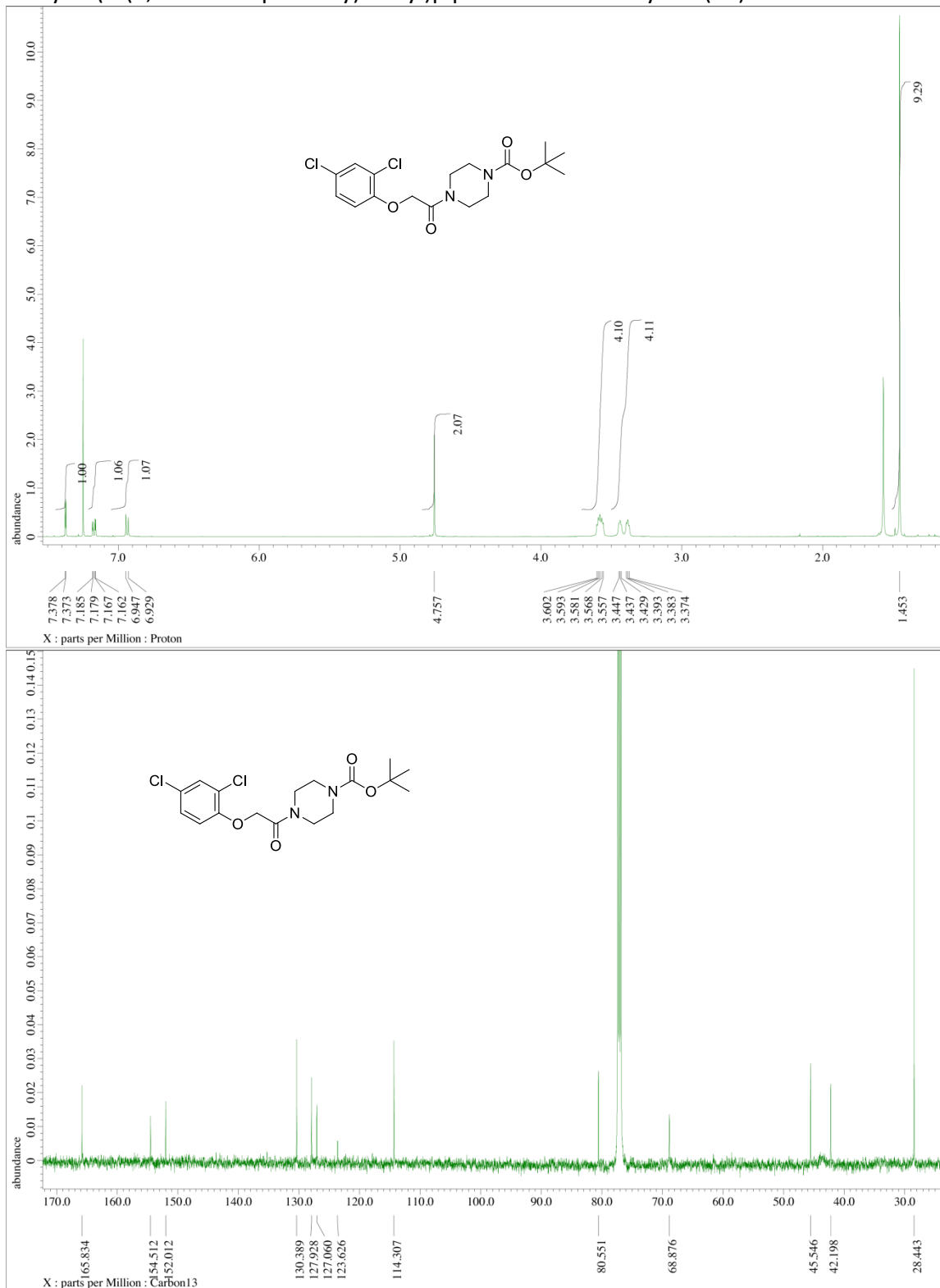


Scheme III

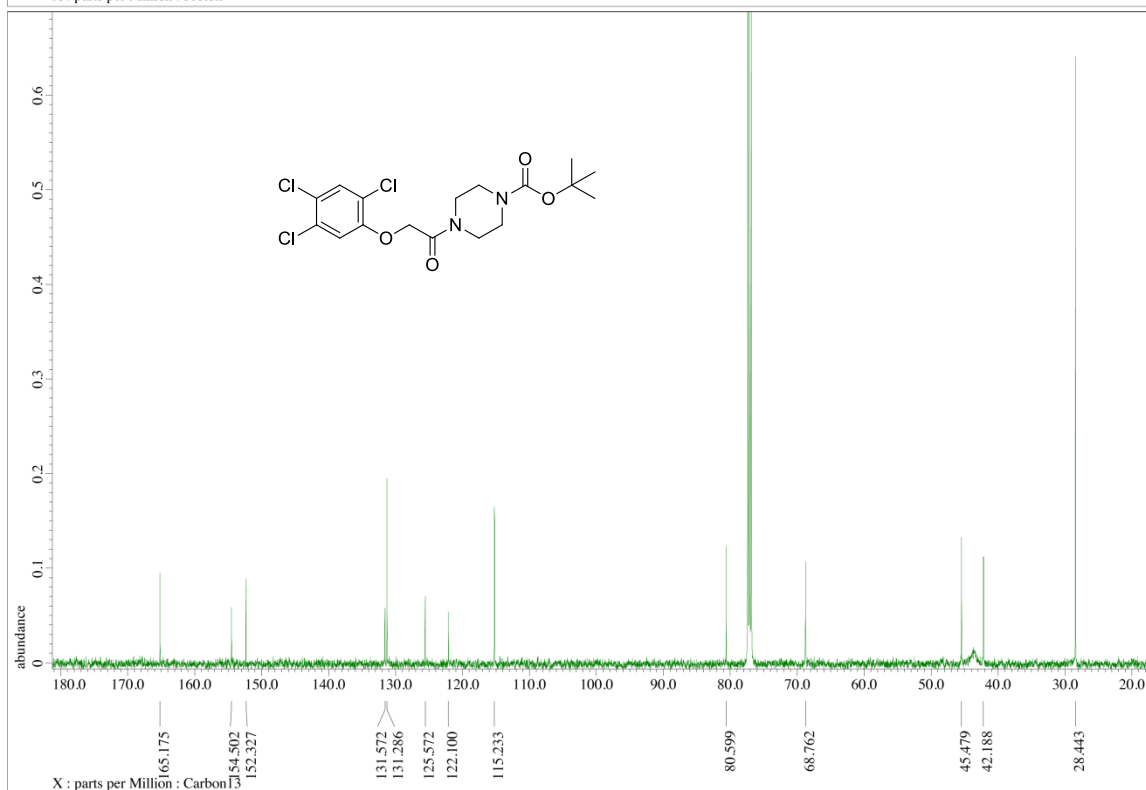
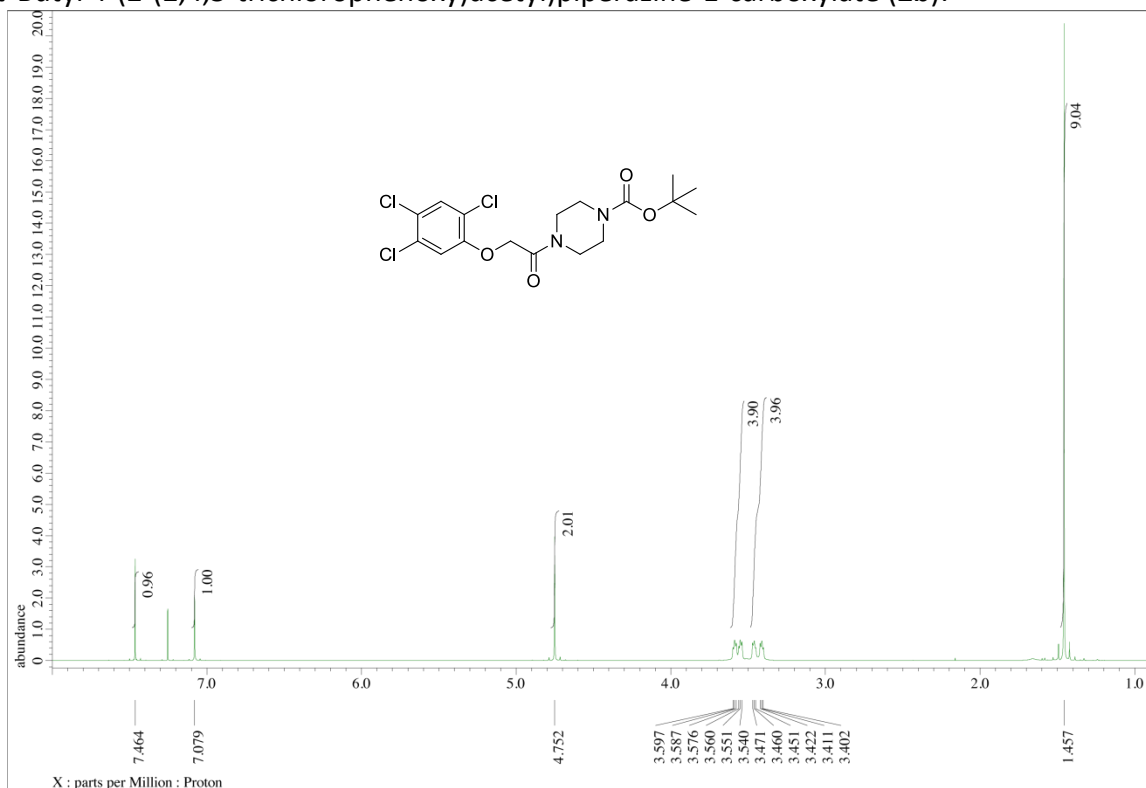
S-(3-((7-Nitrobenzo[c][1,2,5]oxadiazol-4-yl)thio)propyl) 2-(2,4-dichlorophenoxy)ethanethioate
(6, FluorA III): orange solid, $R_f = 0.31$ (petroleum ether/CH₂Cl₂/acetone 30/20/1), yield 20%. ¹H
 NMR (500 MHz, CDCl₃): δ 8.39 (d, $J = 7.95$ Hz, 1H), 7.43 – 7.40 (m, 1H), 7.20 – 7.15 (m, 2H), 6.80
 (d, $J = 8.9$ Hz, 1H), 4.73 (s, 2H), 3.33 (t, $J = 7.3$ Hz, 2H), 3.14 (t, $J = 7.0$ Hz, 2H), 2.14 (p, $J = 7.2$ Hz,
 2H). ¹³C NMR (126 MHz, CDCl₃): δ 197.1, 152.0, 149.3, 142.6, 140.7, 133.0, 130.6 ($\times 2$), 127.8,
 127.7, 124.3, 121.0, 114.6, 73.5, 30.5, 28.1, 26.9. MS (ESI⁻): m/z (%) = 472.0234 ([M-H]⁻, 100).
 HPLC purity: 99.49%.

1.5. ¹H and ¹³C NMR spectra of compounds 2a-e, 3a-e, 4a-e, 5a-e, 6.

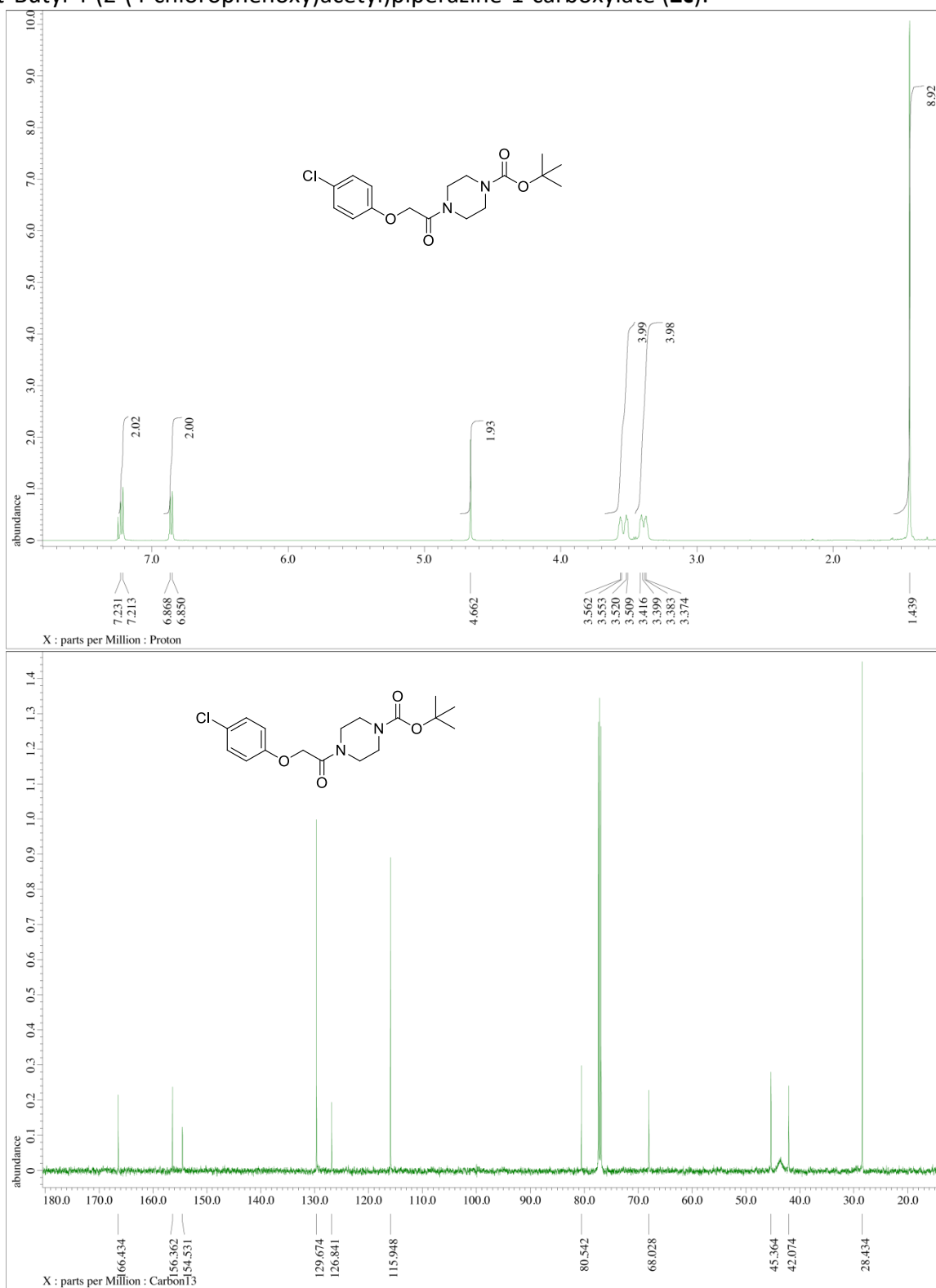
tert-Butyl 4-(2-(2,4-dichlorophenoxy)acetyl)piperazine-1-carboxylate (**2a**):



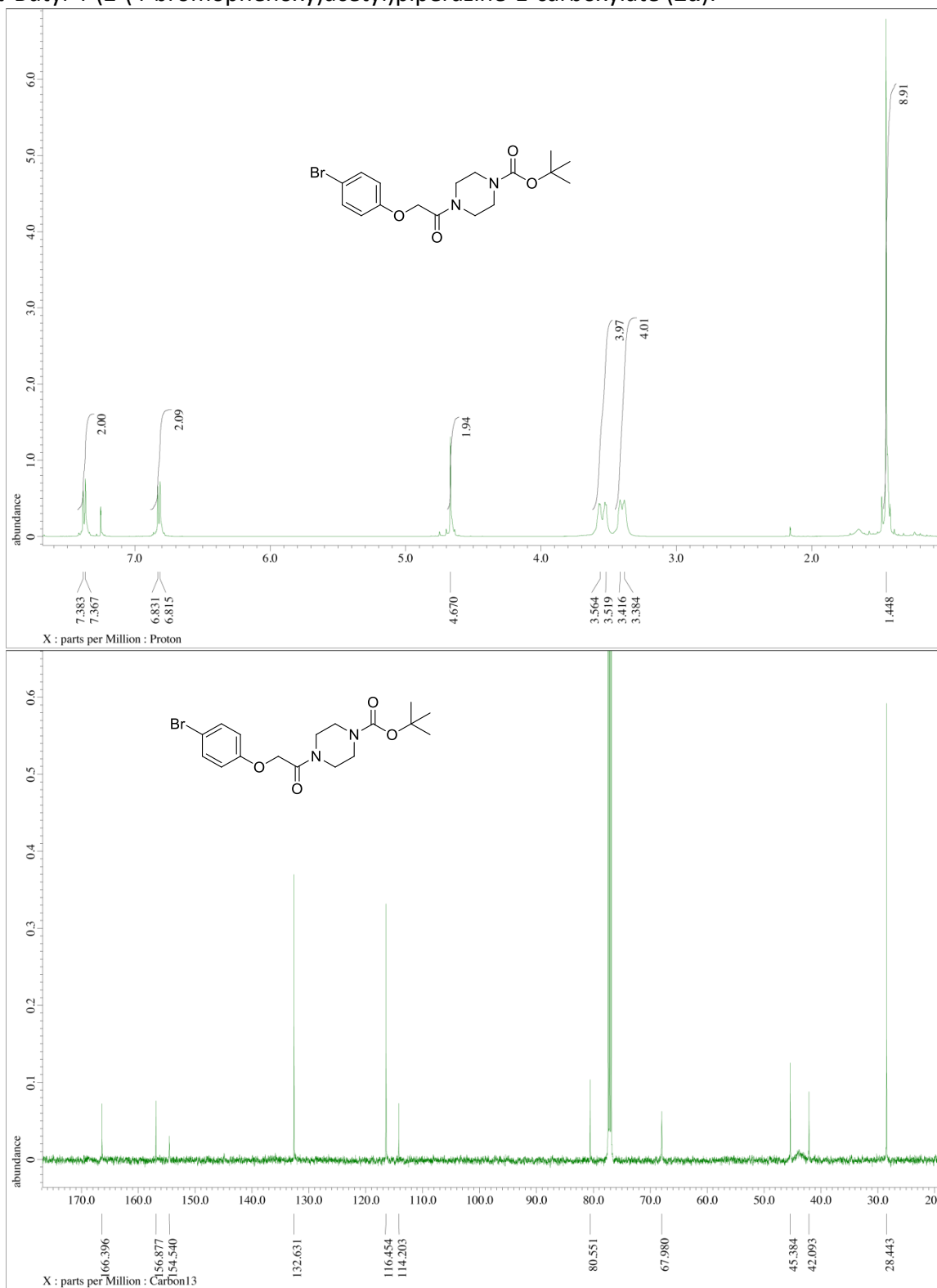
tert-Butyl 4-(2-(2,4,5-trichlorophenoxy)acetyl)piperazine-1-carboxylate (**2b**):



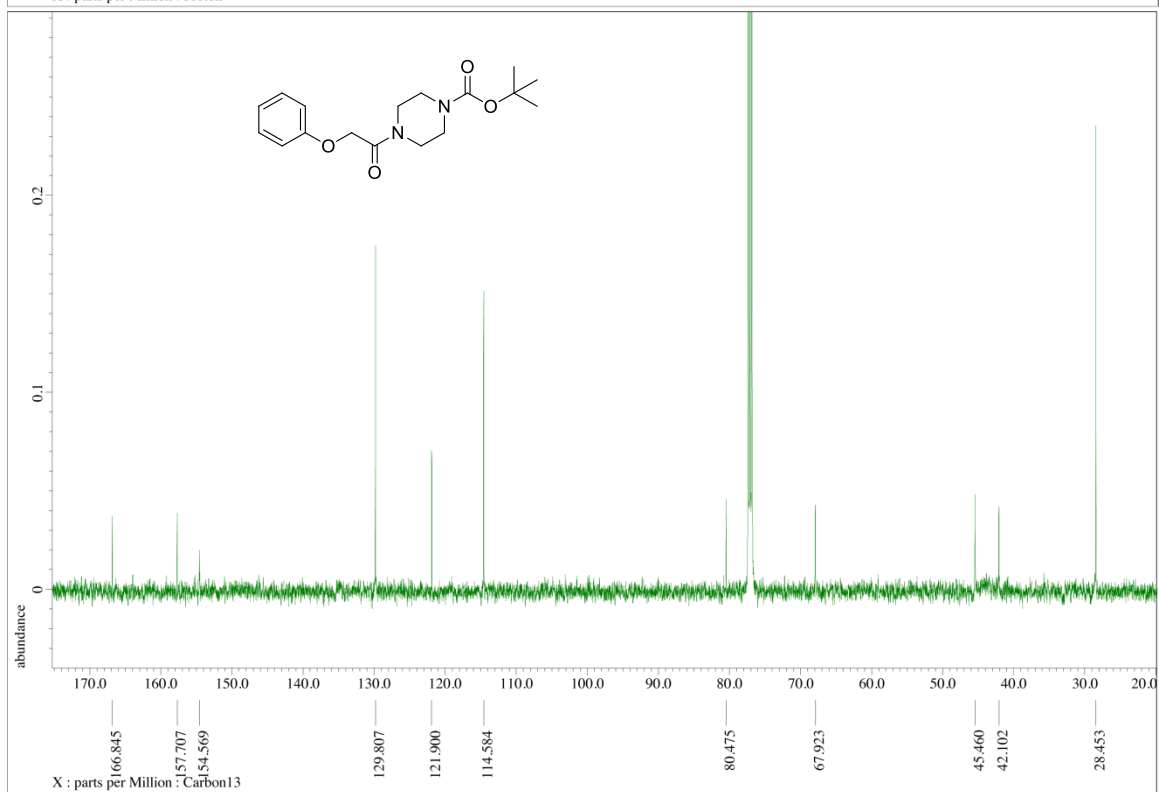
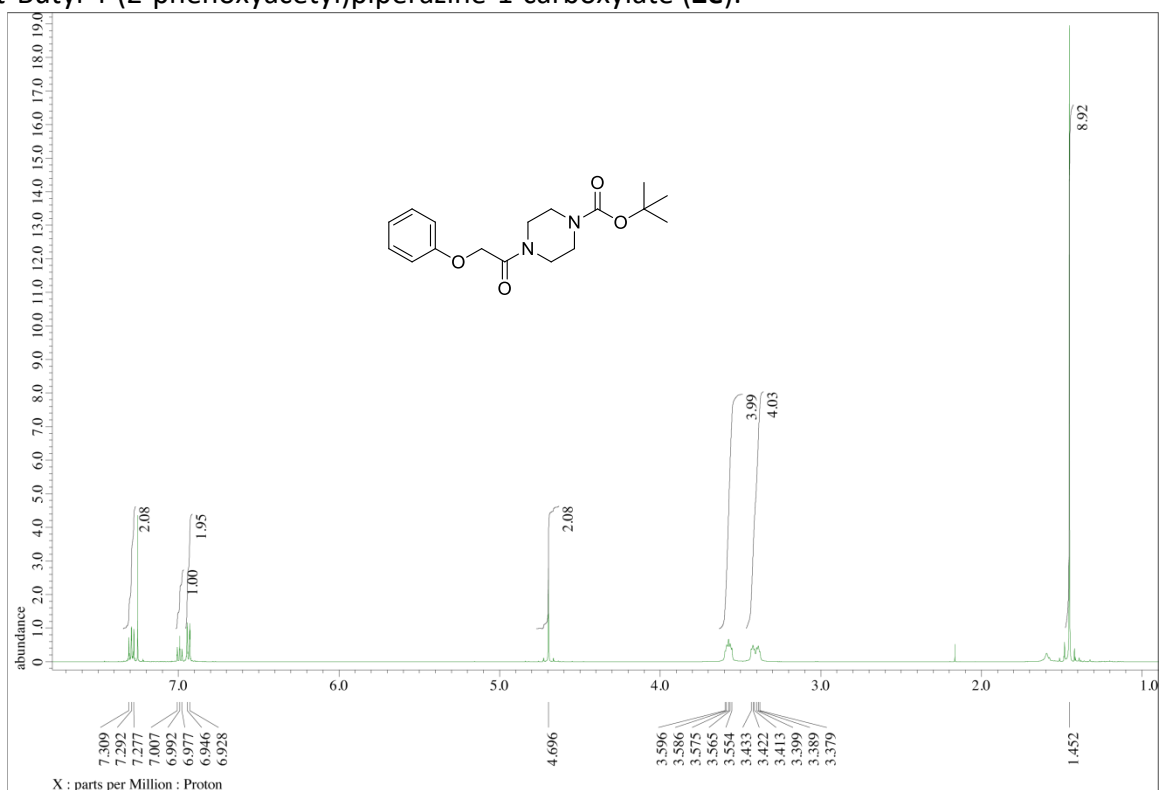
tert-Butyl 4-(2-(4-chlorophenoxy)acetyl)piperazine-1-carboxylate (**2c**):



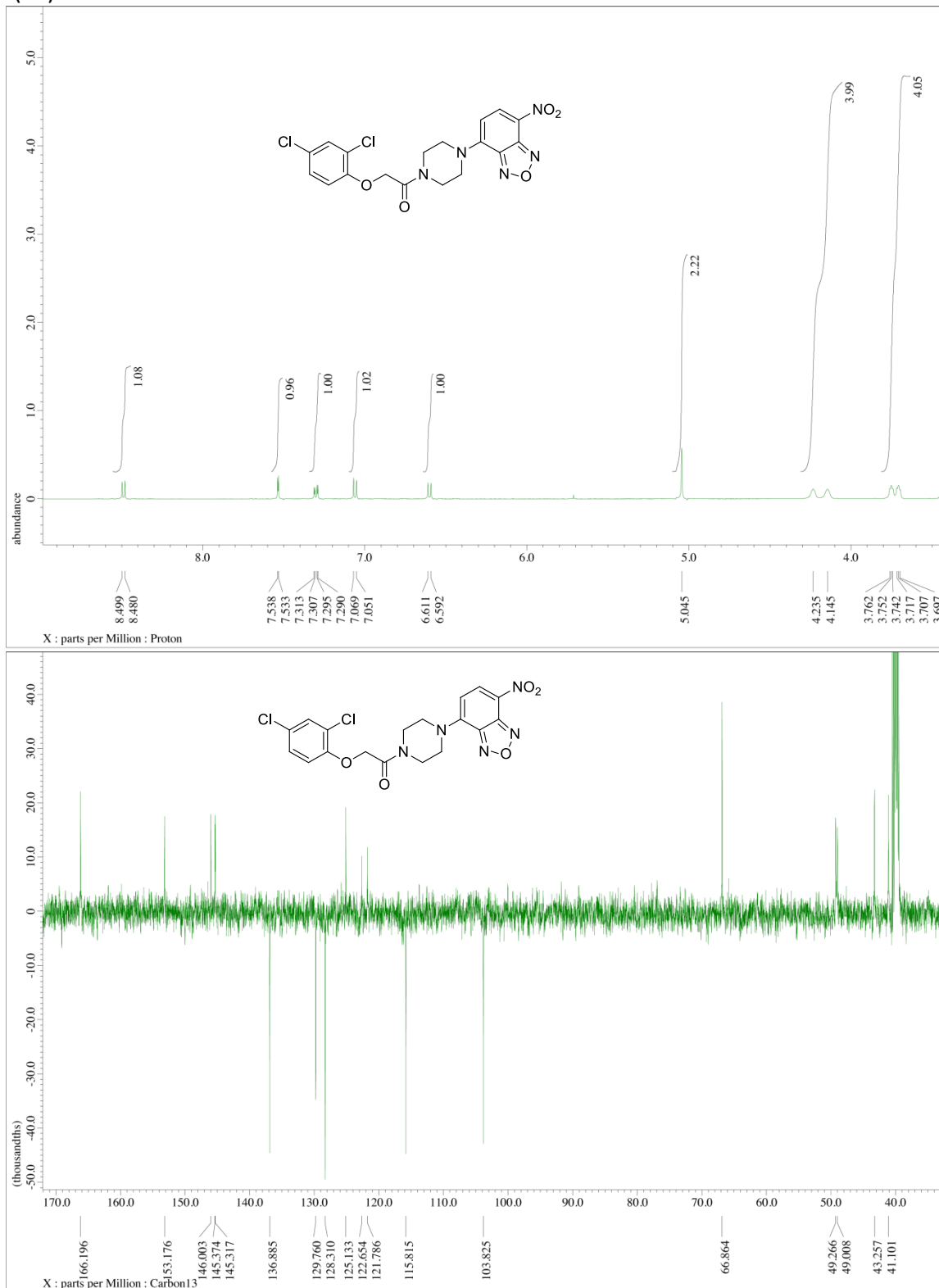
tert-Butyl 4-(2-(4-bromophenoxy)acetyl)piperazine-1-carboxylate (**2d**):



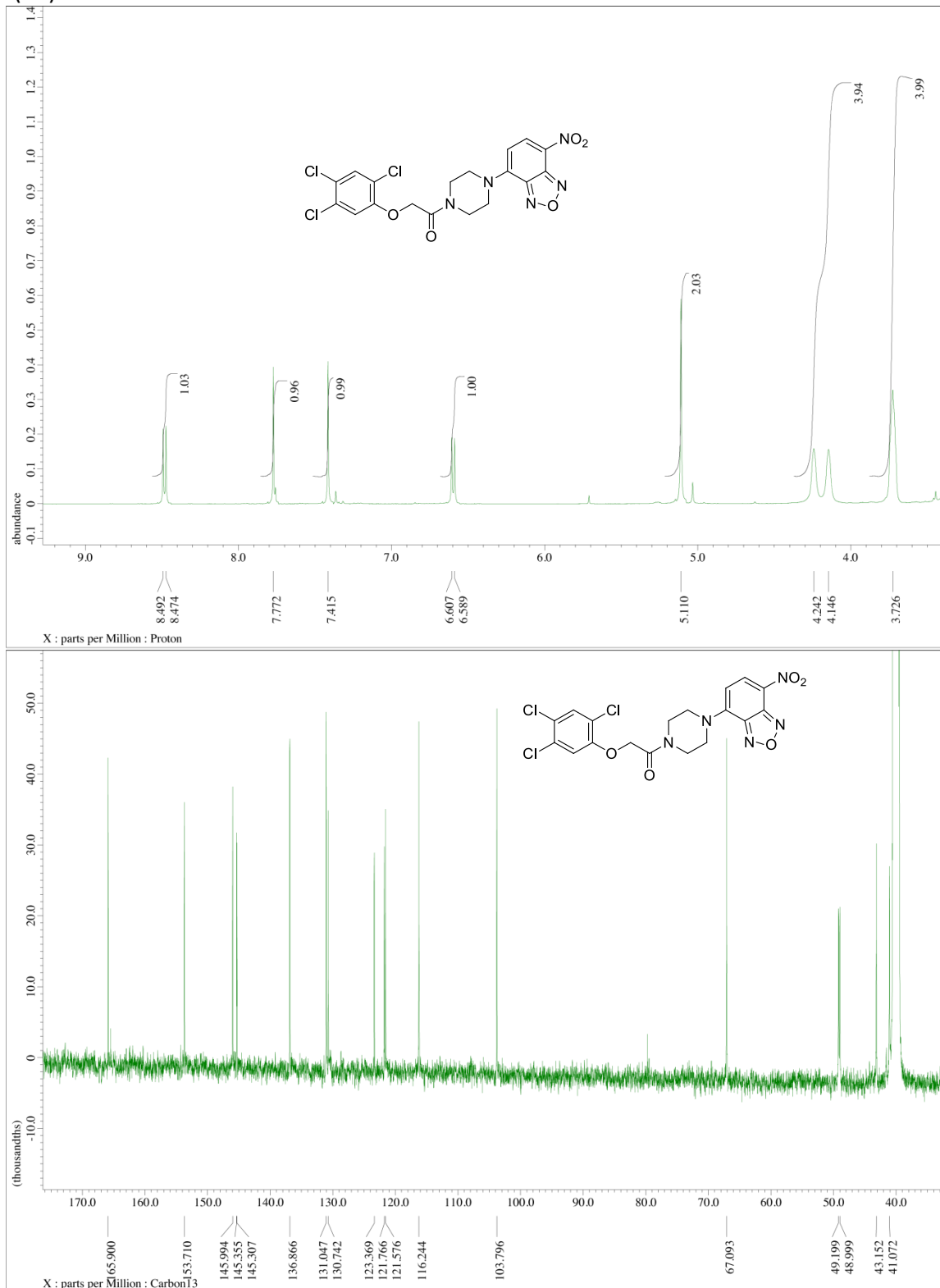
tert-Butyl 4-(2-phenoxyacetyl)piperazine-1-carboxylate (**2e**):



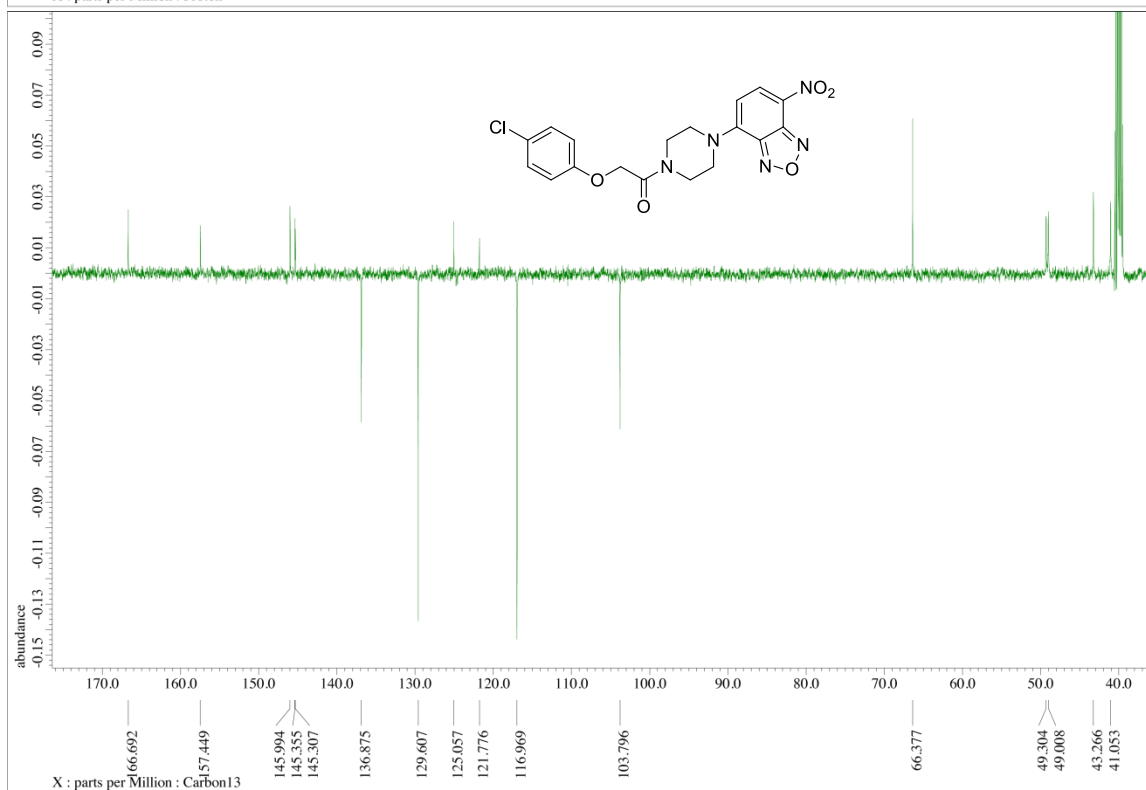
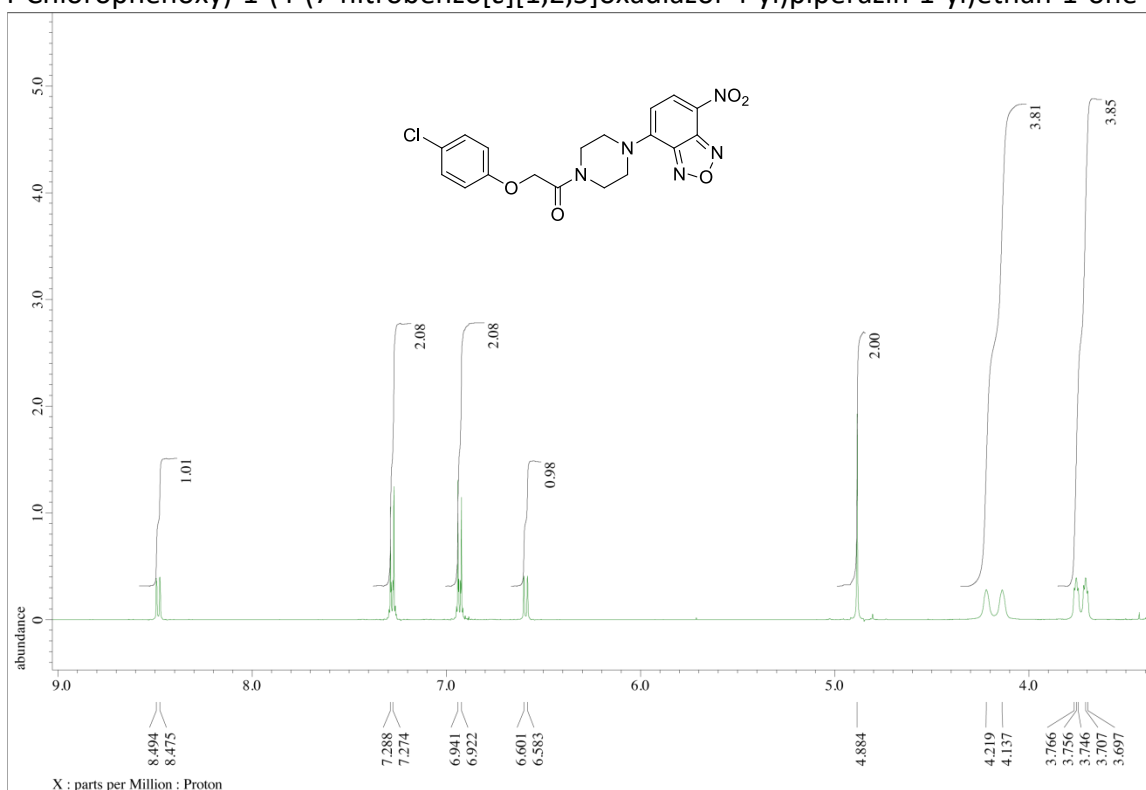
2-(2,4-Dichlorophenoxy)-1-(4-(7-nitrobenzo[c][1,2,5]oxadiazol-4-yl)piperazin-1-yl)ethan-1-one (**3a**):



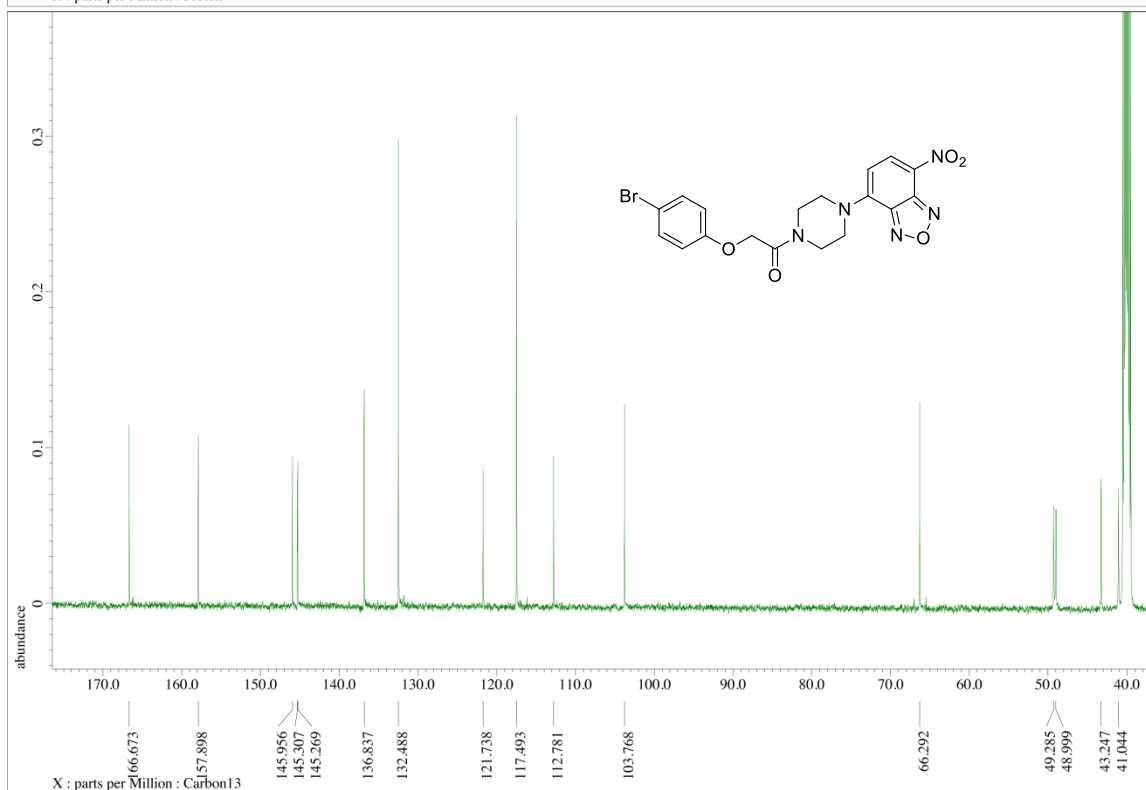
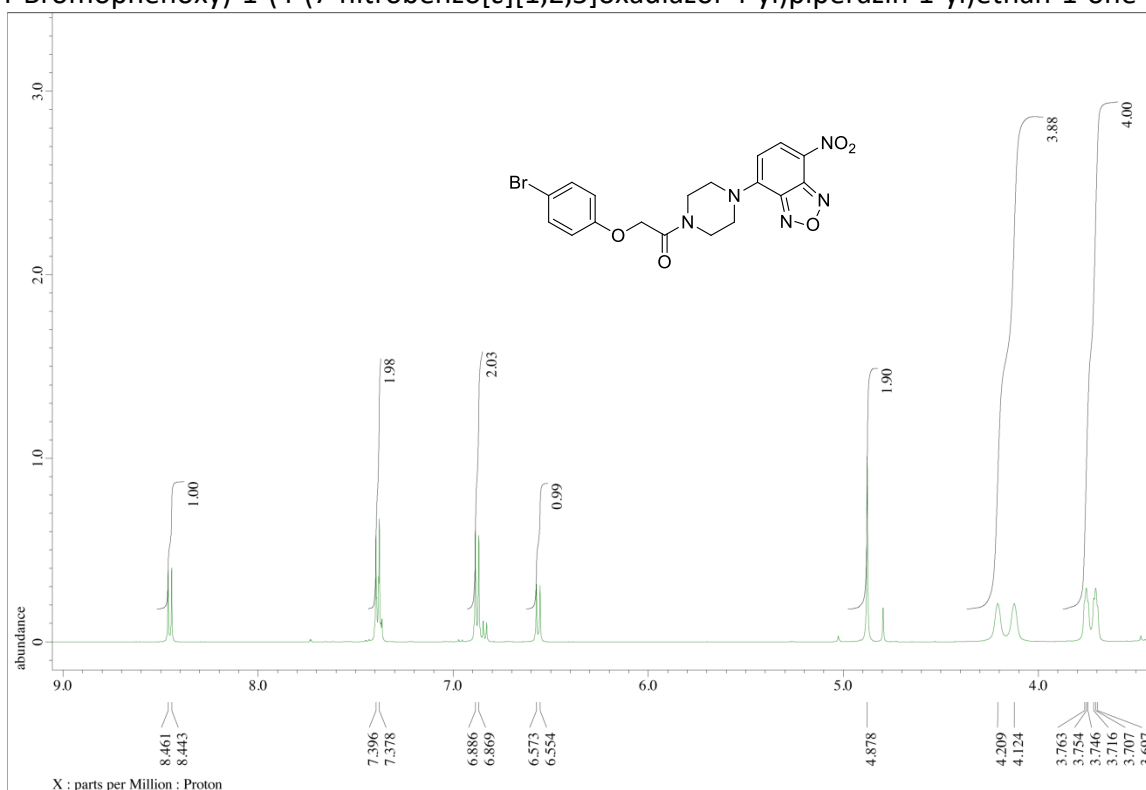
1-(4-(7-Nitrobenzo[c][1,2,5]oxadiazol-4-yl)piperazin-1-yl)-2-(2,4,5-trichlorophenoxy)ethan-1-one (**3b**):



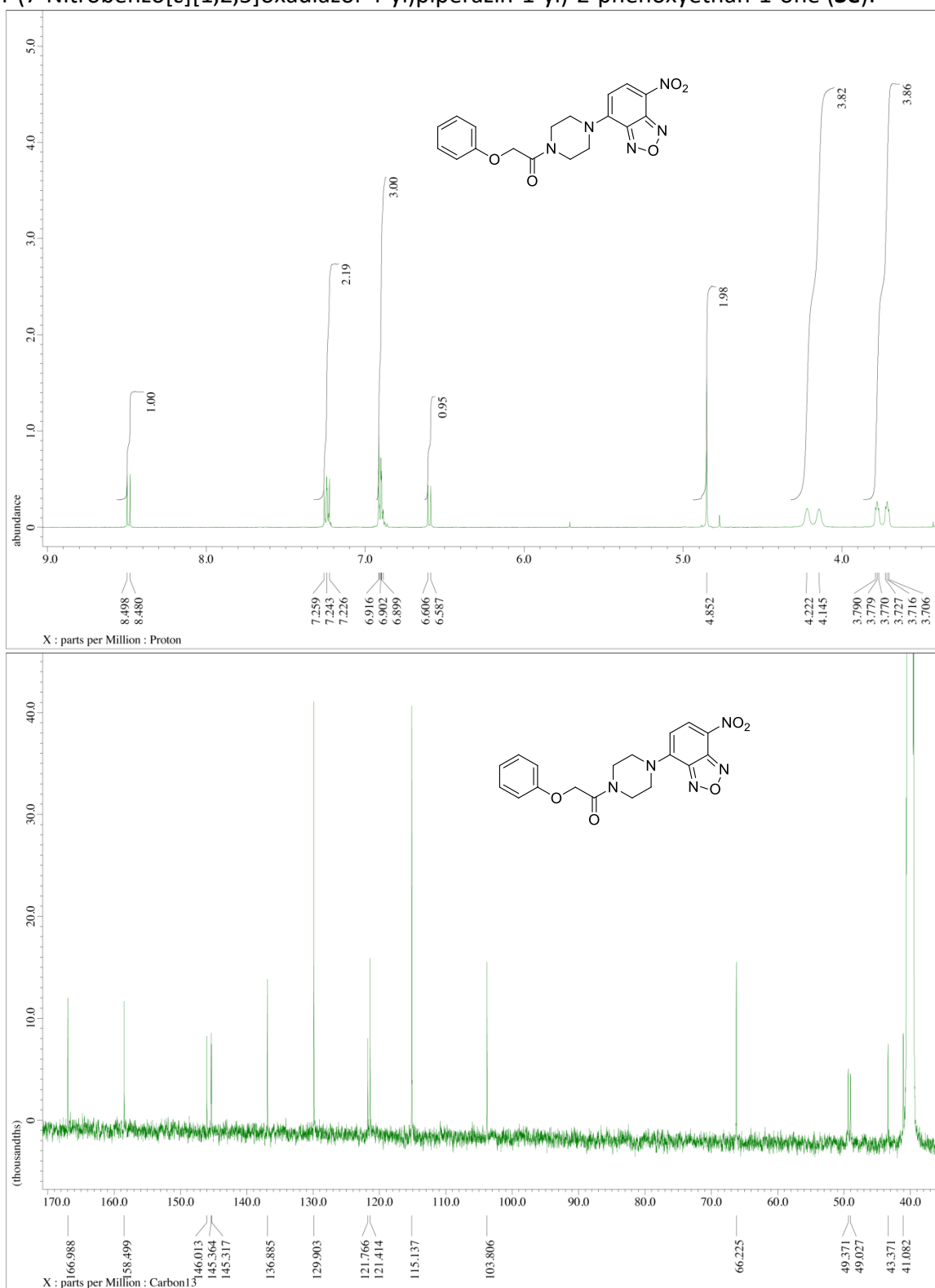
2-(4-Chlorophenoxy)-1-(4-(7-nitrobenzo[c][1,2,5]oxadiazol-4-yl)piperazin-1-yl)ethan-1-one (**3c**):



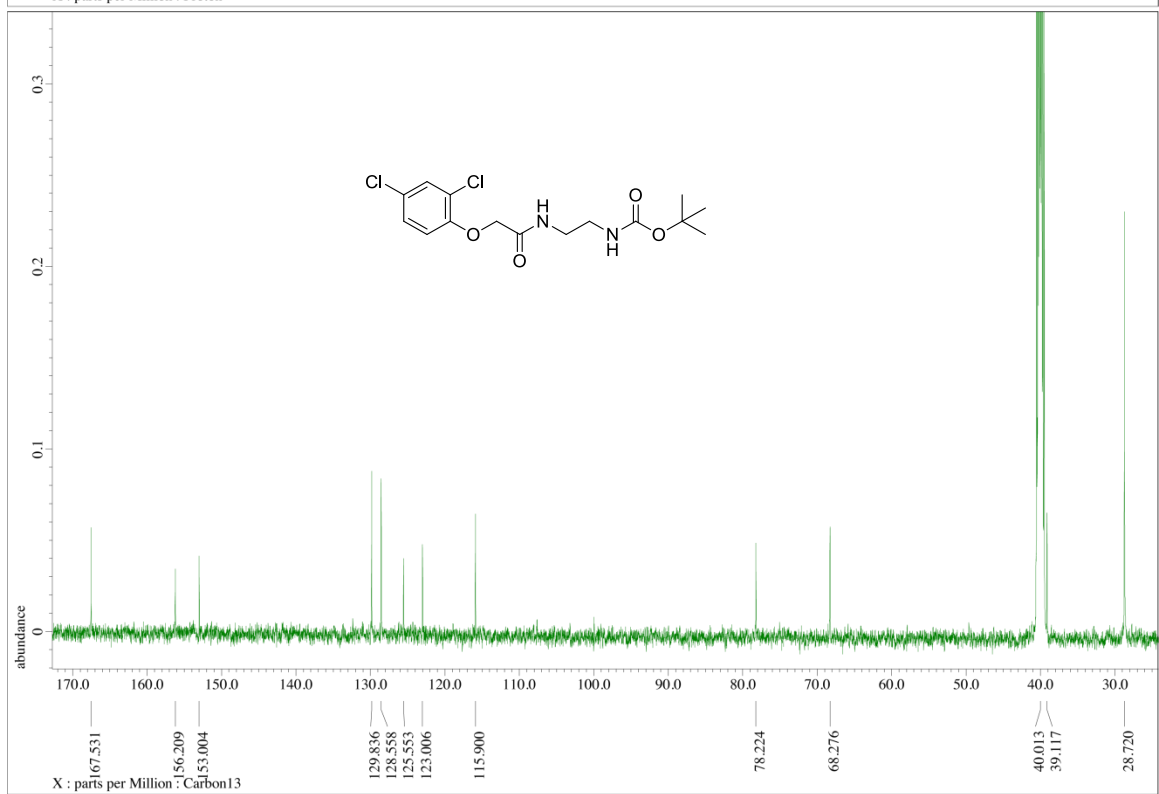
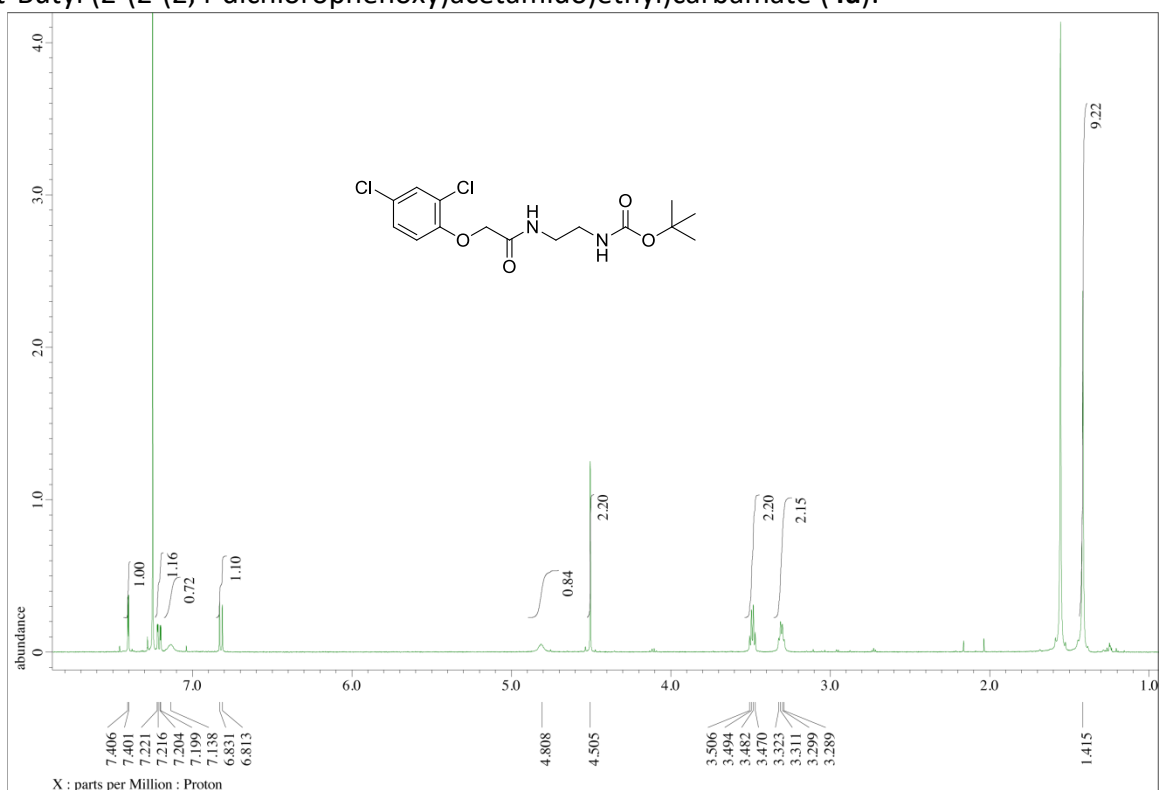
2-(4-Bromophenoxy)-1-(4-(7-nitrobenzo[c][1,2,5]oxadiazol-4-yl)piperazin-1-yl)ethan-1-one (**3d**):



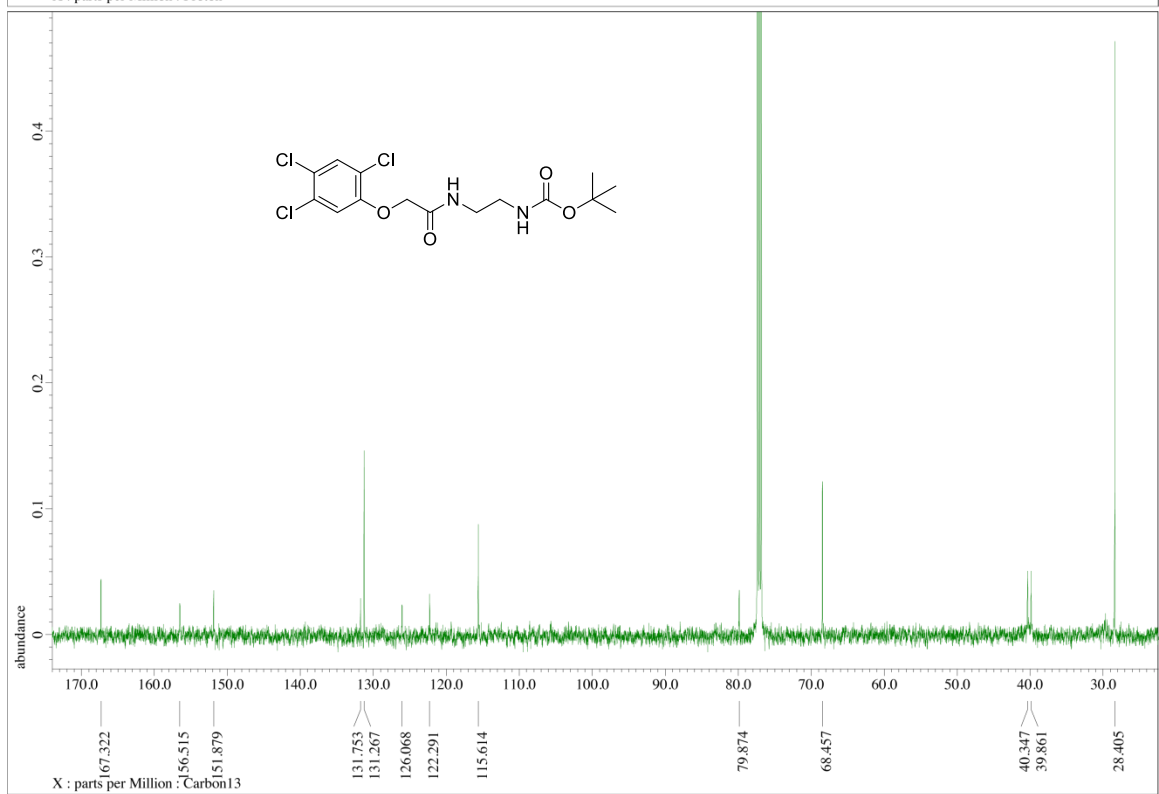
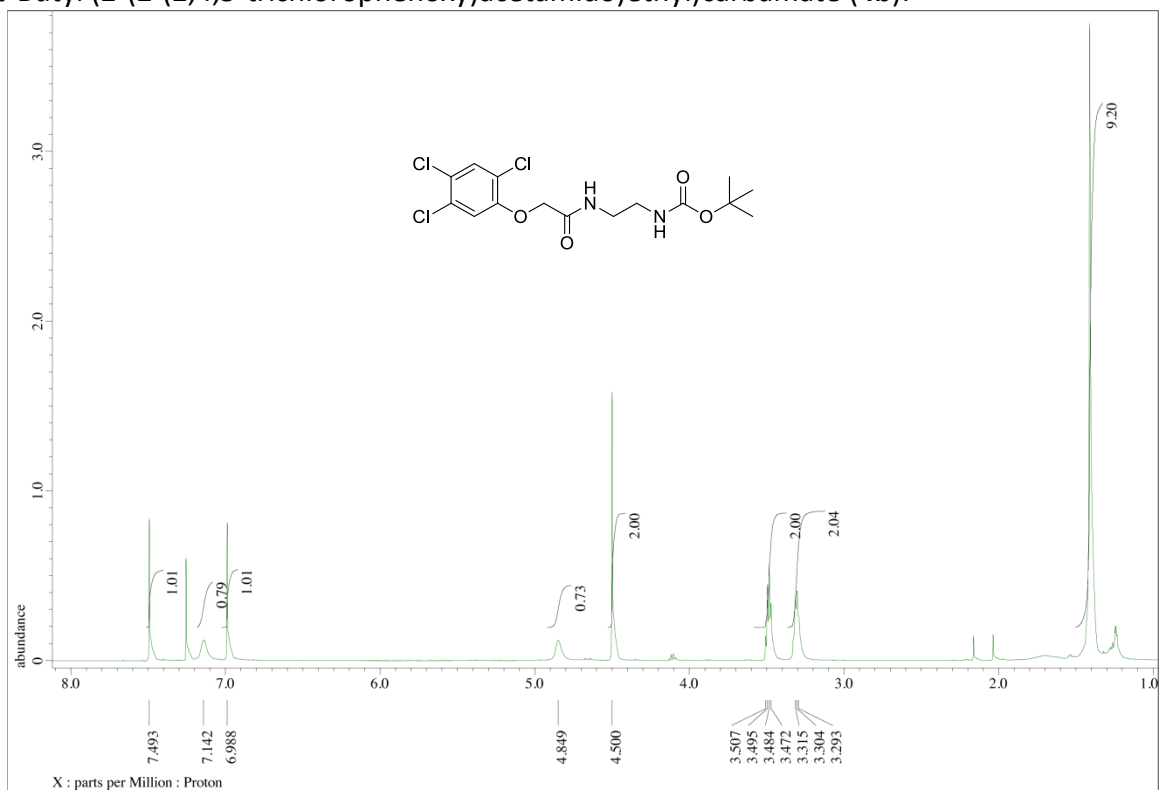
1-(4-(7-Nitrobenzo[c][1,2,5]oxadiazol-4-yl)piperazin-1-yl)-2-phenoxyethan-1-one (**3e**):



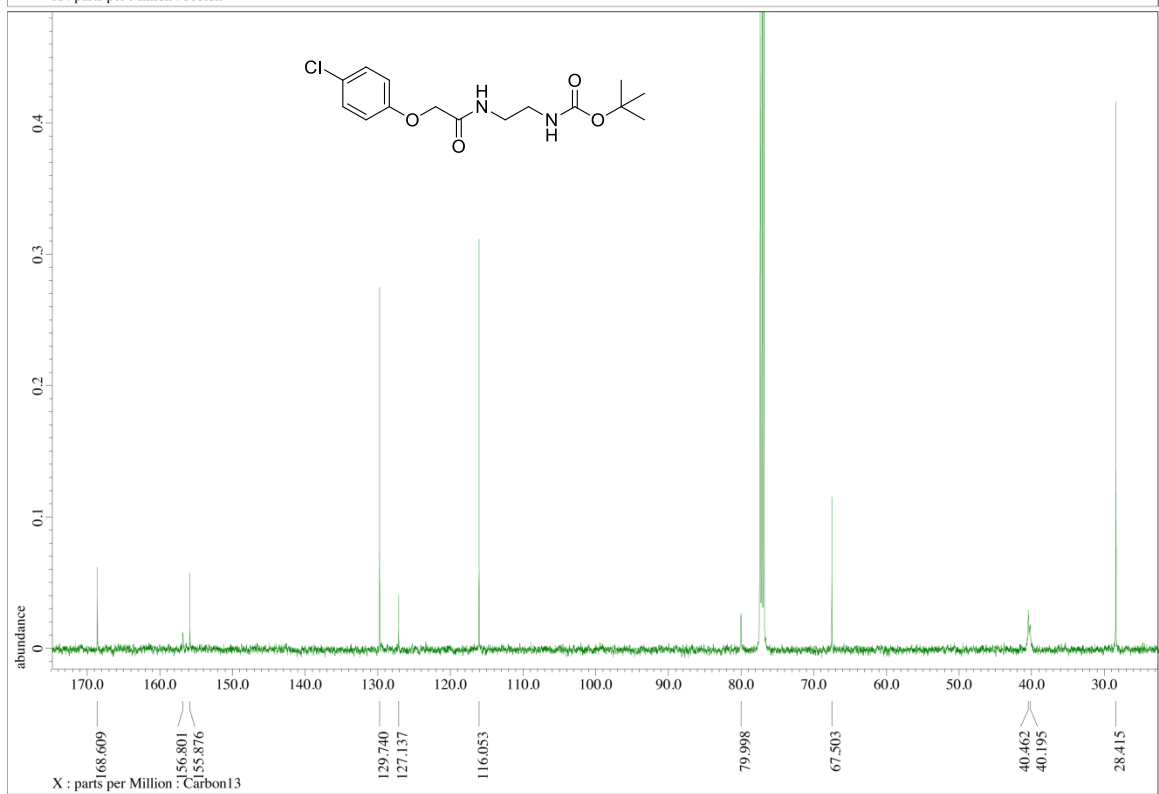
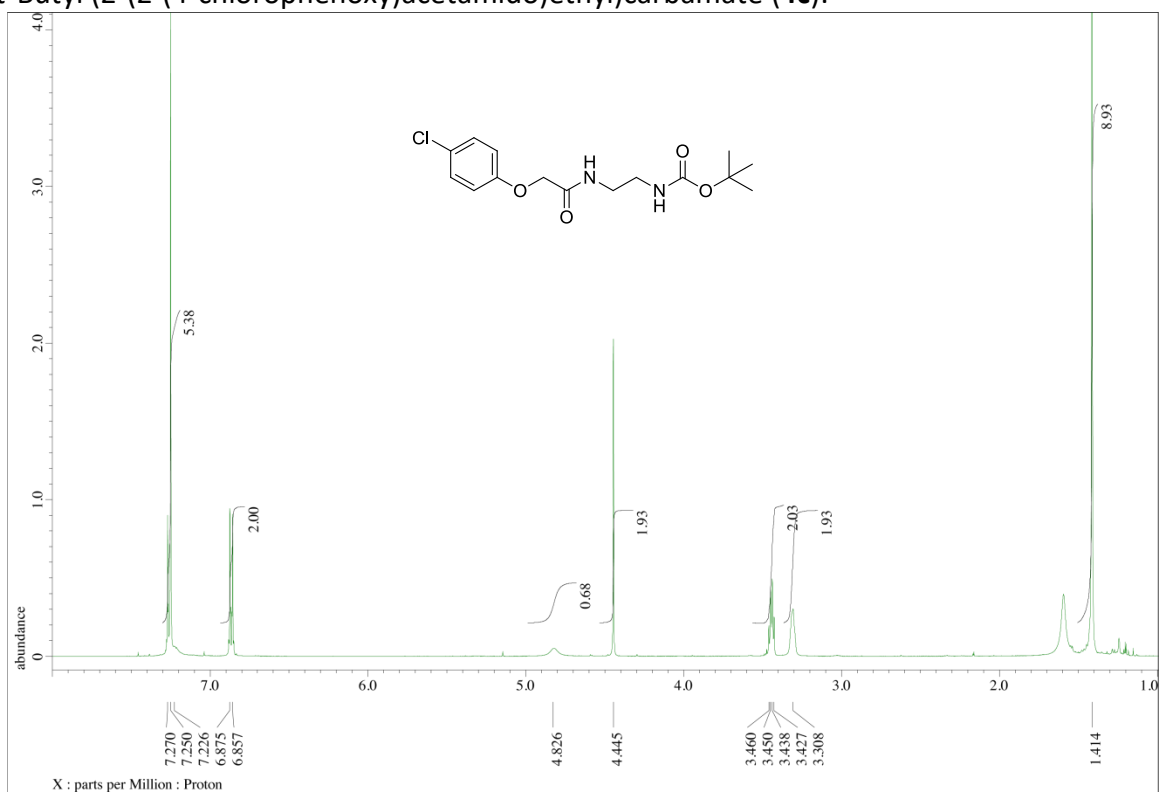
tert-Butyl (2-(2-(2,4-dichlorophenoxy)acetamido)ethyl)carbamate (**4a**):



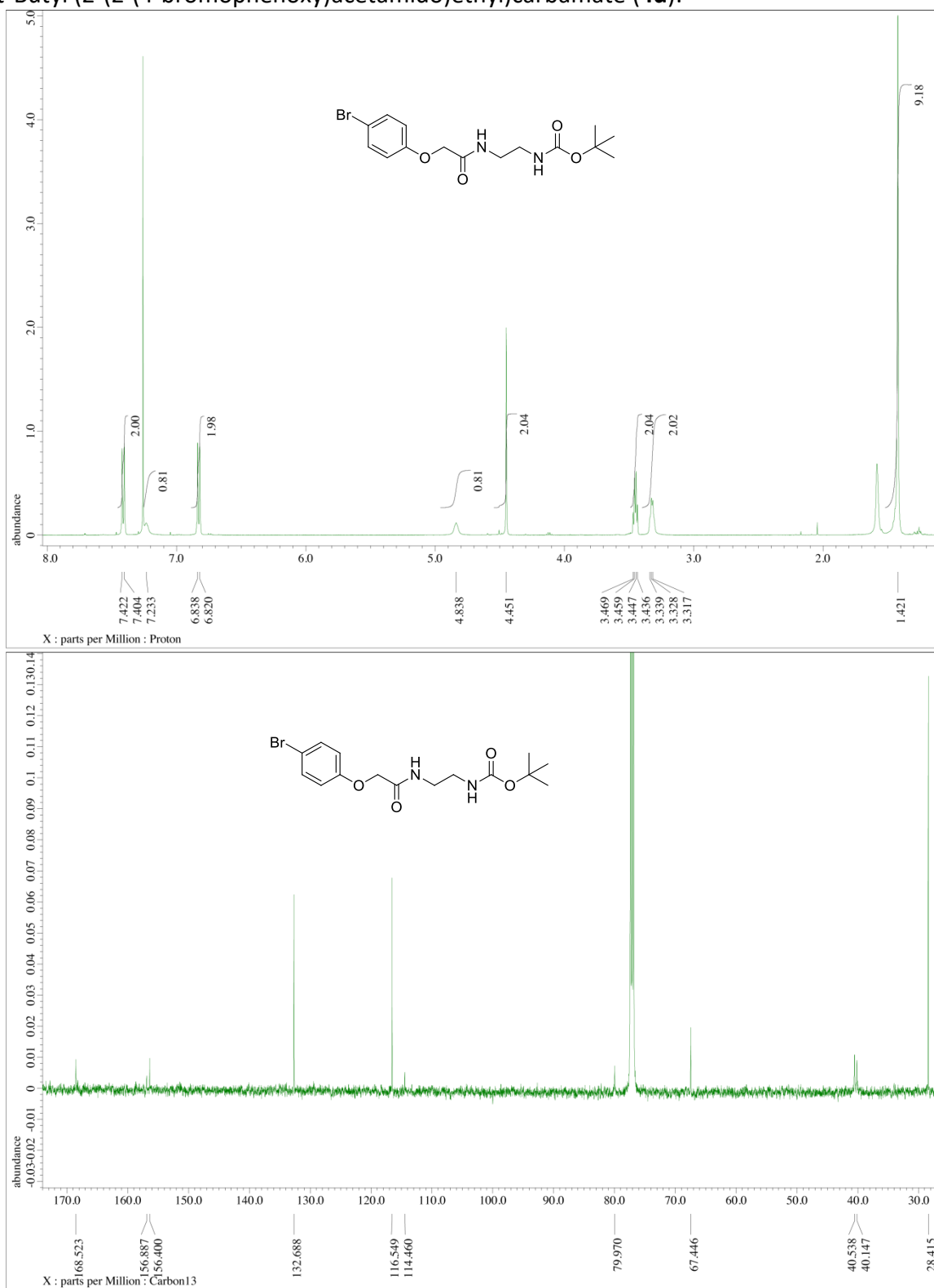
tert-Butyl (2-(2-(2,4,5-trichlorophenoxy)acetamido)ethyl)carbamate (**4b**):



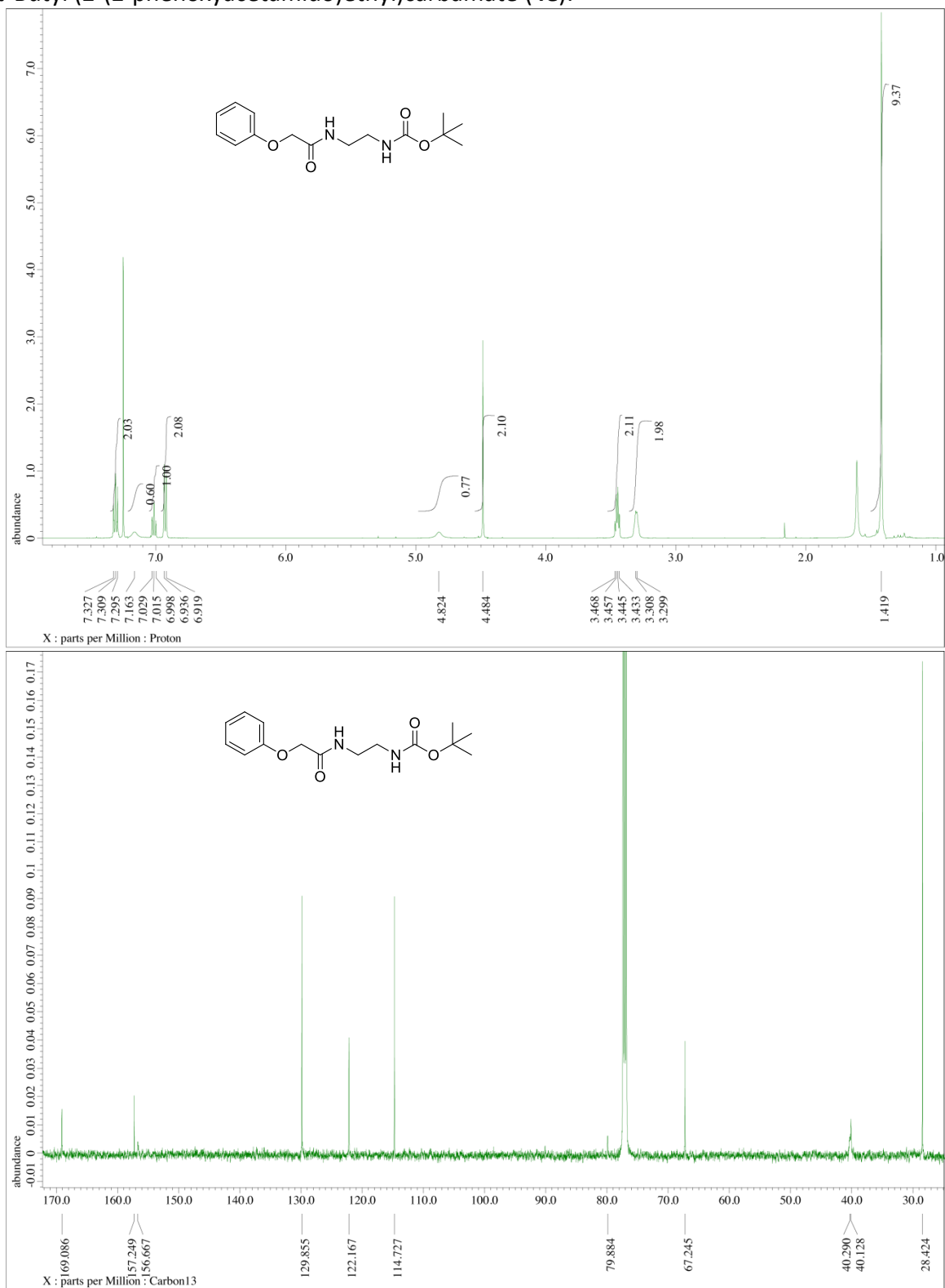
tert-Butyl 2-(2-(4-chlorophenoxy)acetamido)ethylcarbamate (**4c**):



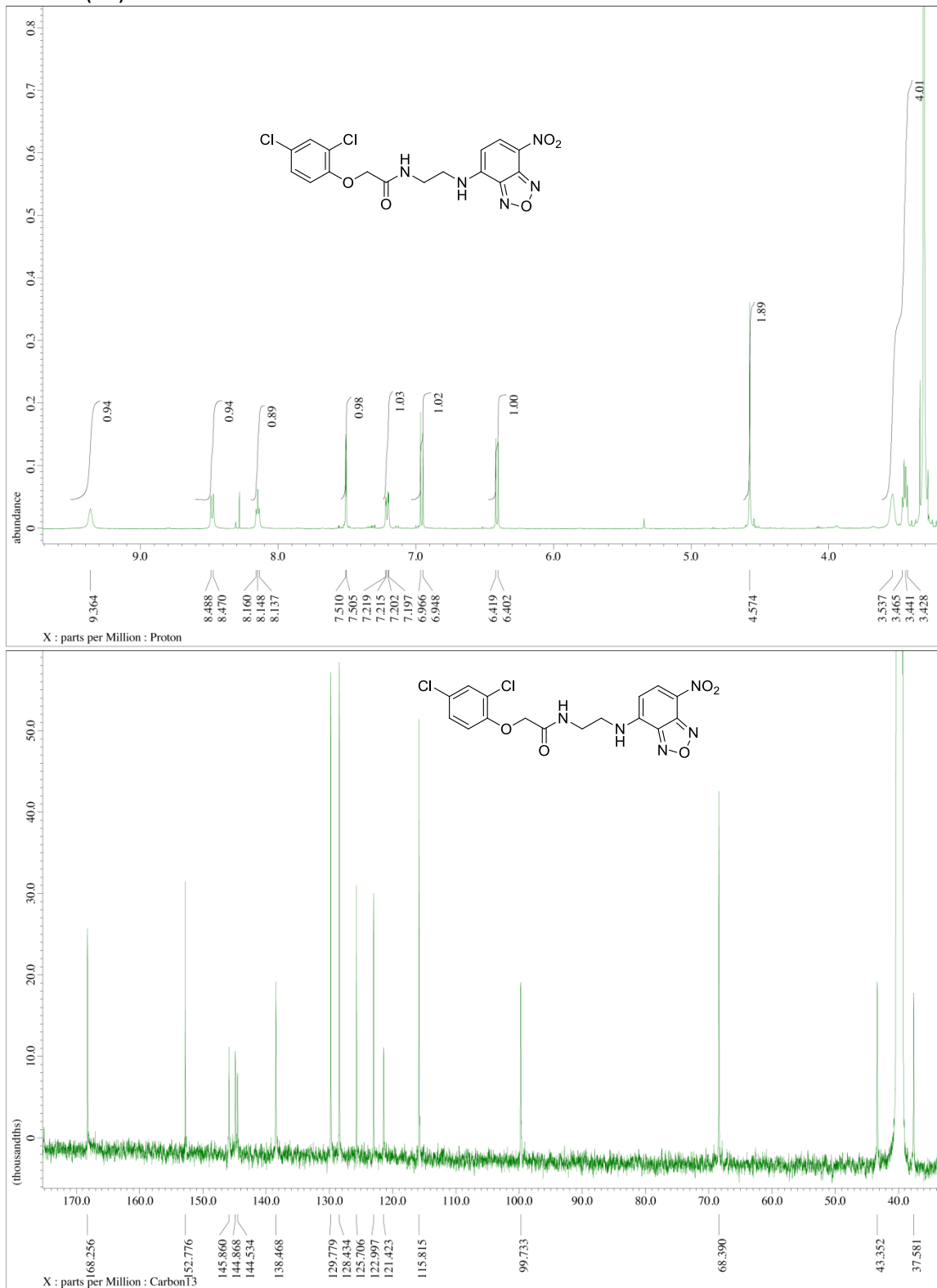
tert-Butyl (2-(2-(4-bromophenoxy)acetamido)ethyl)carbamate (**4d**):



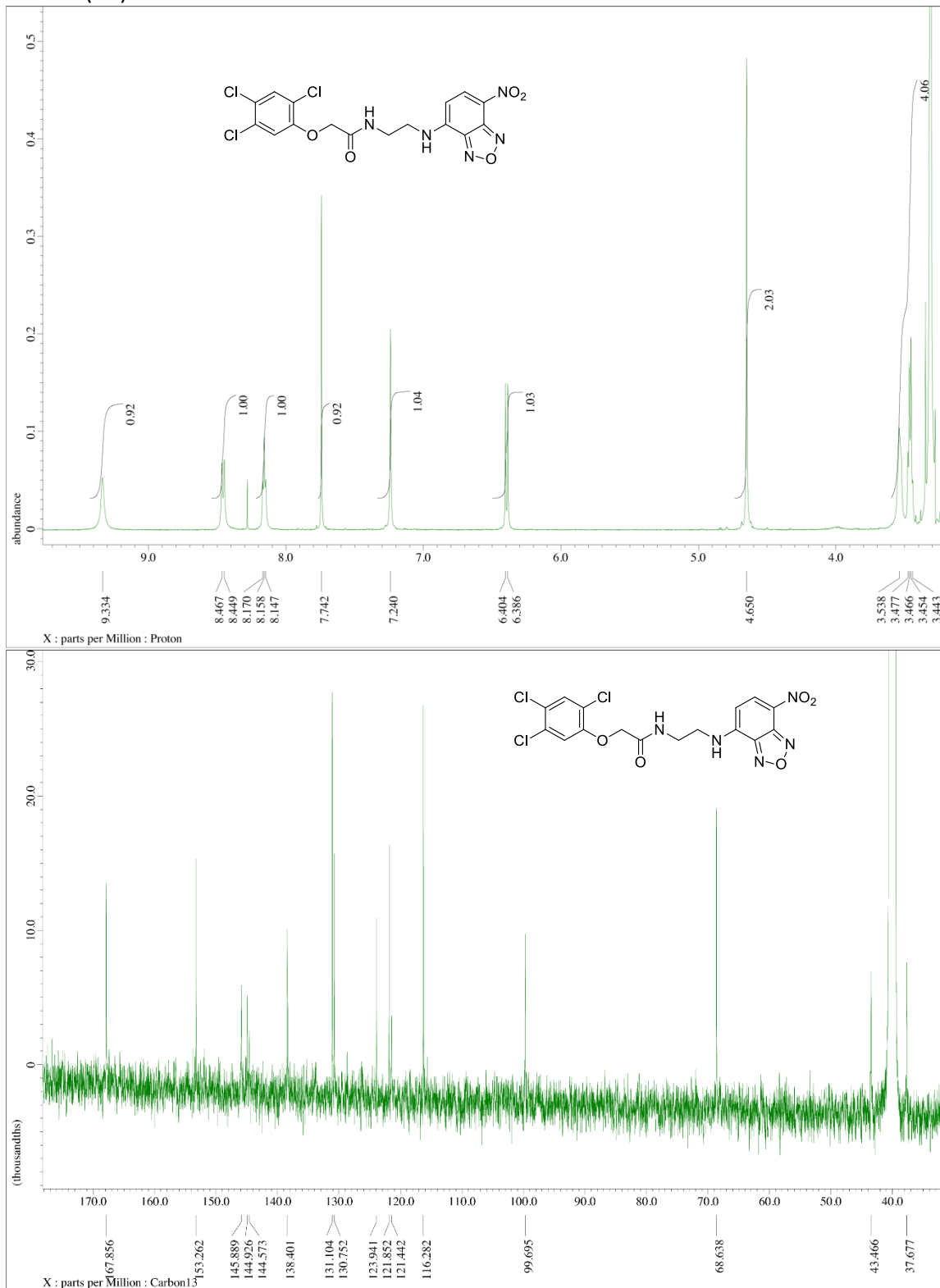
tert-Butyl (2-(2-phenoxyacetamido)ethyl)carbamate (**4e**):



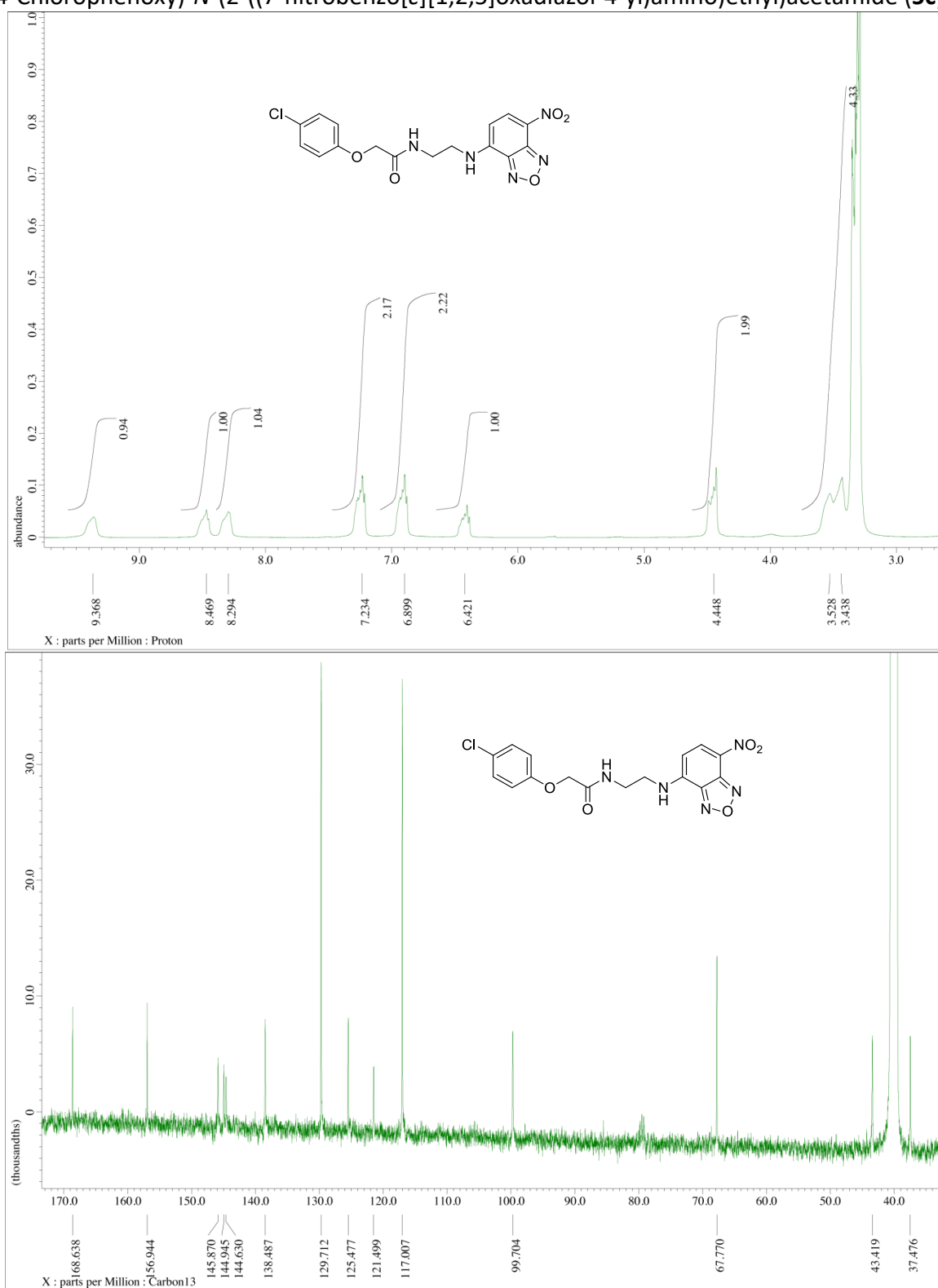
2-(2,4-Dichlorophenoxy)-*N*-((7-nitrobenzo[*c*][1,2,5]oxadiazol-4-yl)amino)ethyl)acetamide (**5a**):



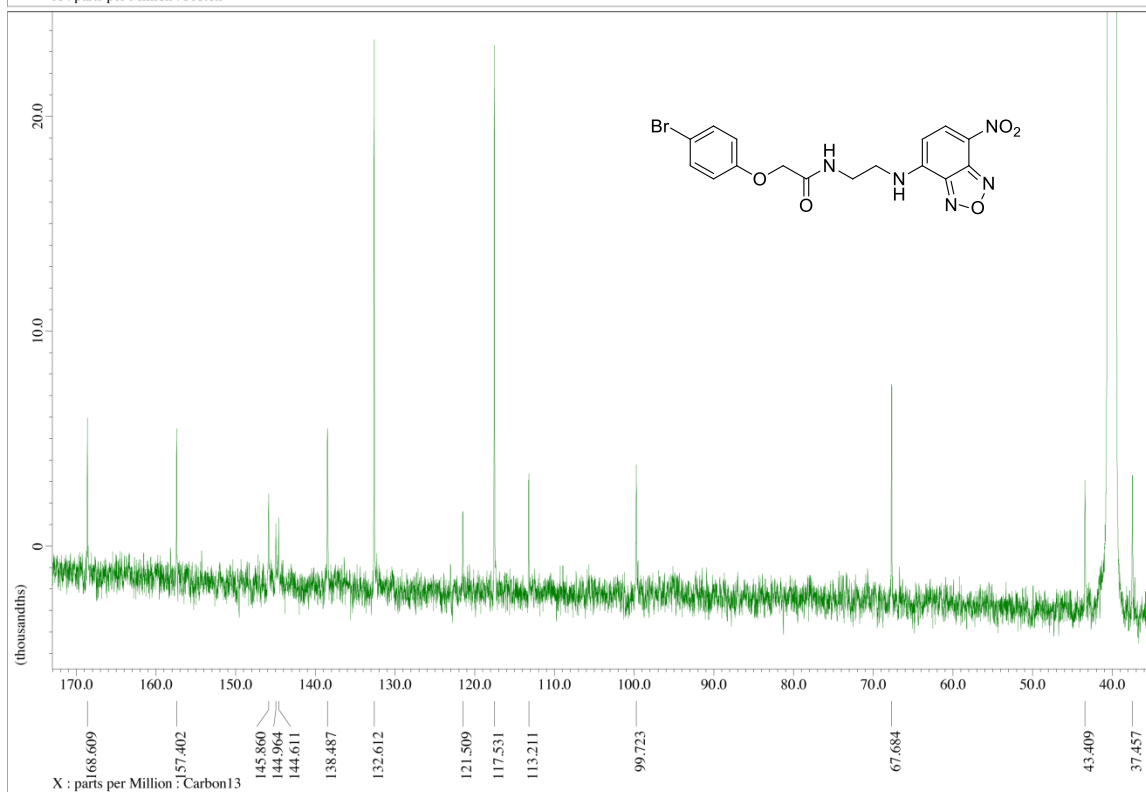
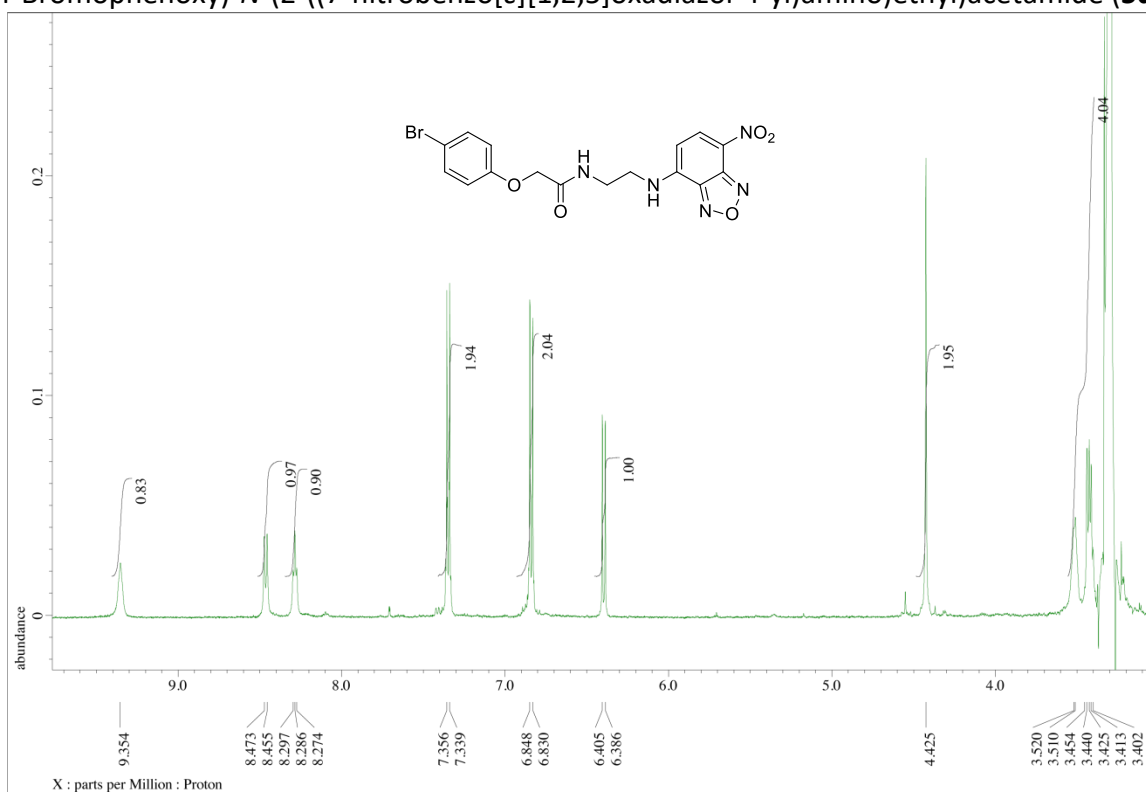
N-(2-((7-Nitrobenzo[*c*][1,2,5]oxadiazol-4-yl)amino)ethyl)-2-(2,4,5-trichlorophenoxy)acetamide (**5b**):



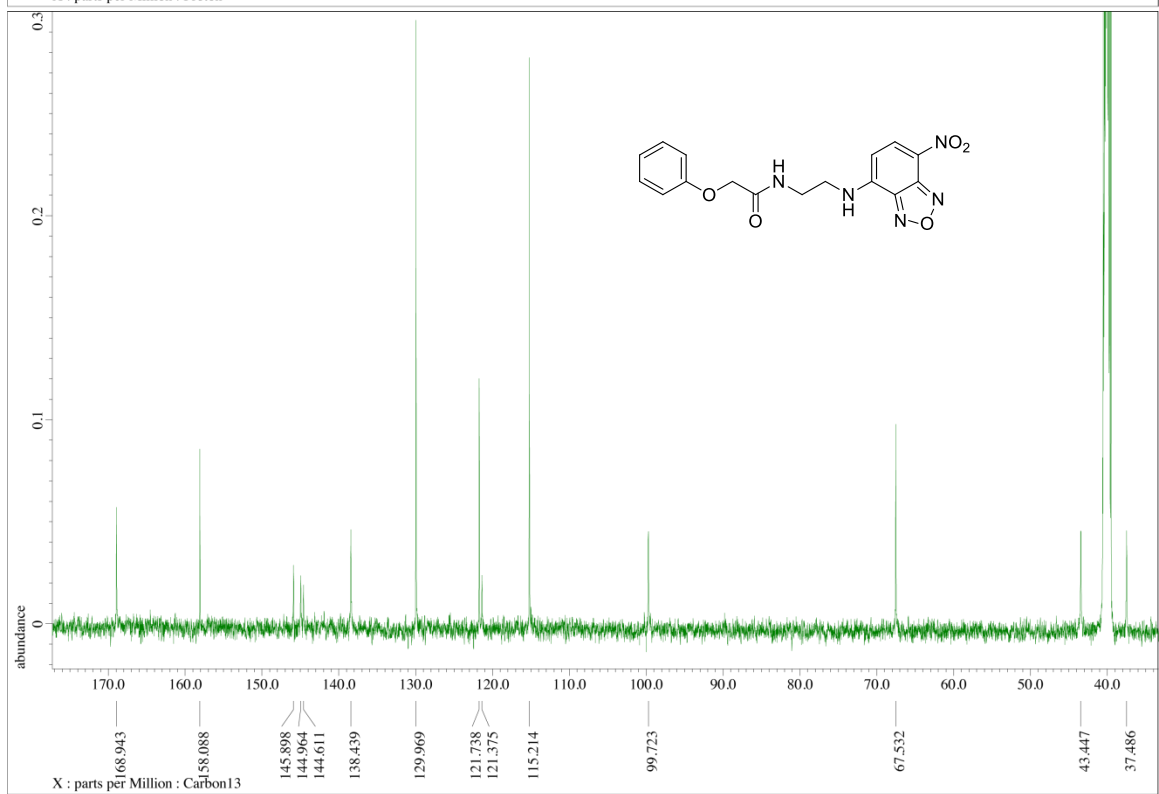
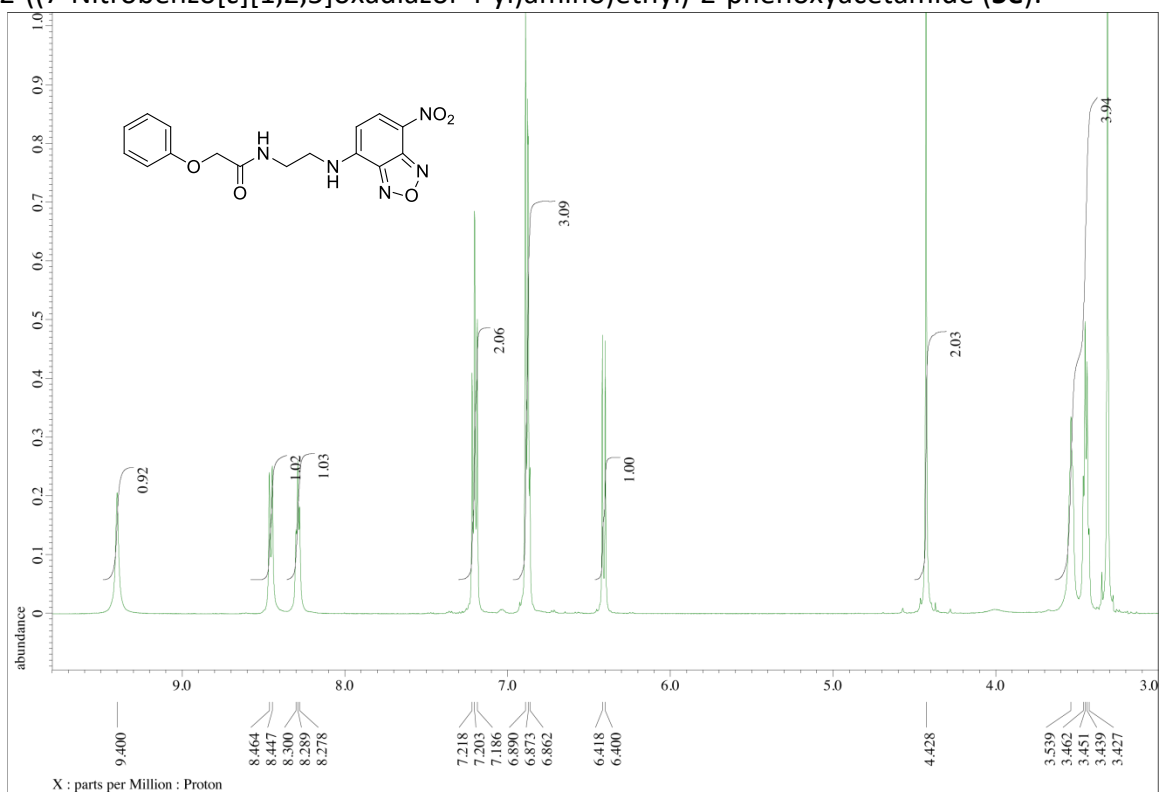
2-(4-Chlorophenoxy)-N-(2-((7-nitrobenzo[c][1,2,5]oxadiazol-4-yl)amino)ethyl)acetamide (**5c**):



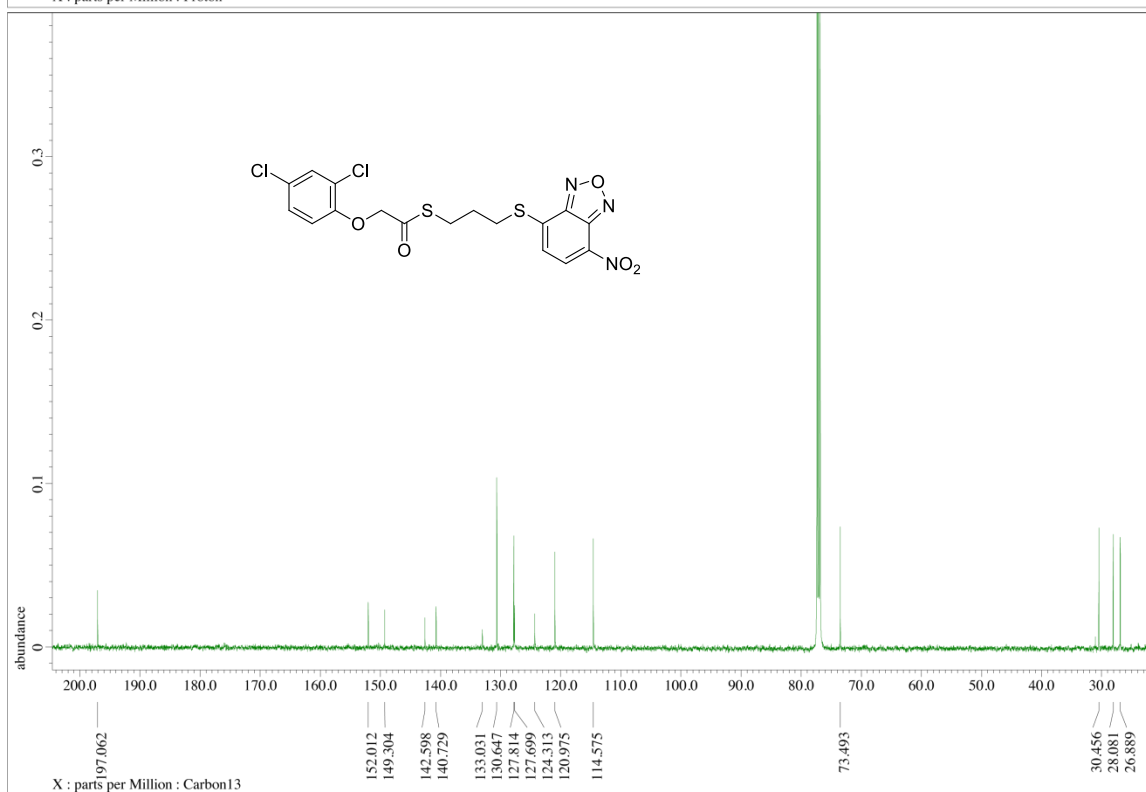
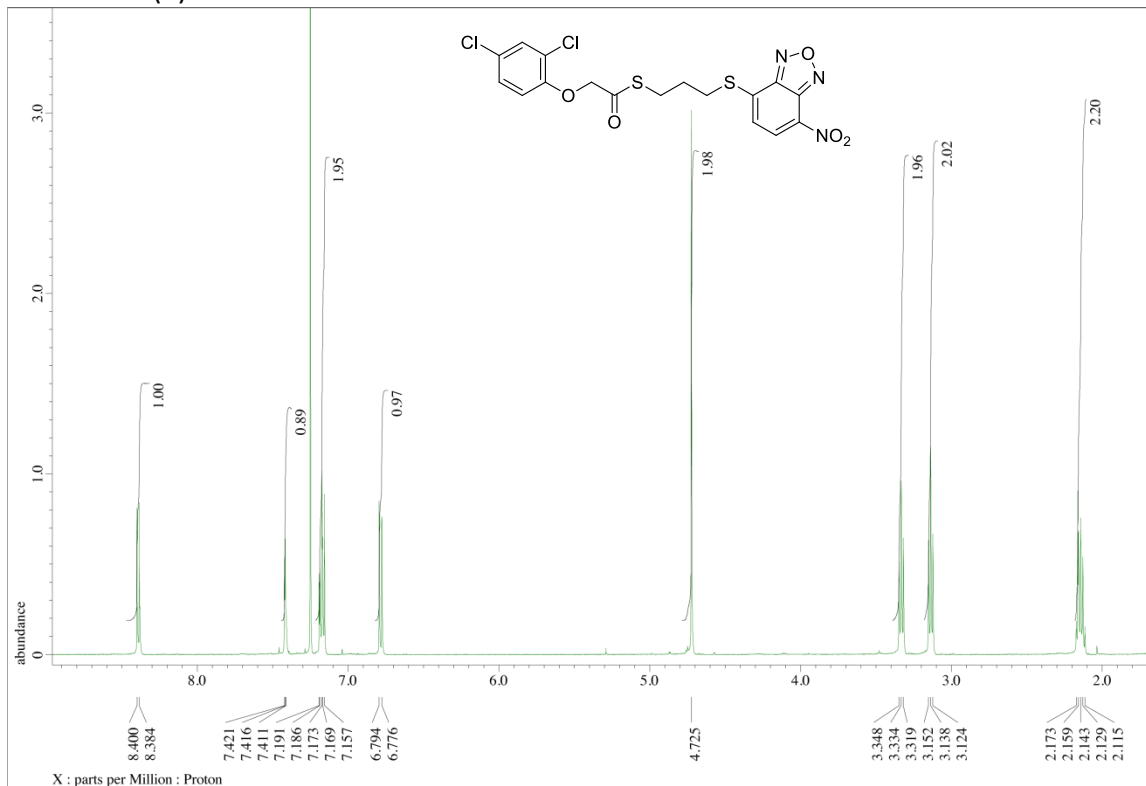
2-(4-Bromophenoxy)-*N*-((7-nitrobenzo[*c*][1,2,5]oxadiazol-4-yl)amino)ethyl)acetamide (**5d**):



N-(2-((7-Nitrobenzo[*c*][1,2,5]oxadiazol-4-yl)amino)ethyl)-2-phenoxyacetamide (**5e**):



S-(3-((7-Nitrobenzo[c][1,2,5]oxadiazol-4-yl)thio)propyl) 2-(2,4-dichlorophenoxy) ethanethioate (**6**):



Methods S2 LC-MS/MS determination of metabolization dynamics.

Five-day-old *Arabidopsis* Col-0 seedlings were transferred to liquid ½ MS medium with 2 µM fluorescent analogues or only DMSO as a control and treated for defined periods of time (0.5 – 3 h). Non-treated plants were used as a control for time-point 0 h. At distinct time-points, the plants were collected and the roots were harvested to obtain 50 roots per one biological replicate, rinsed with fresh medium, frozen in liquid nitrogen and stored at -80 °C until extraction. The one-step purification method based on liquid-liquid extraction was used to remove impurities from the complex plant matrix. Briefly, 900 µl of the extraction solution (hexane:MeOH:H₂O – 1:1:1) was added to plant samples (50 seedlings/sample) together with 2 mm ceria-stabilized zirconium oxide beads. In each extract, 500 pmol of [²H₅]2,4-D (CDN Isotopes, Canada), 1 pmol of [¹³C₂]FluorA I and 10 pmol of [¹³C₂]FluorA II, synthesized from [¹³C₂]2,4-D (Eyer *et al.*, 2016) analogously to that described above for non-labeled conjugates, were added as internal standards to validate the determination. Homogenization was performed using a MixerMill MM 301 bead mill (Retsch GmbH, Haan, Deutschland) for 3 x 3 minutes at a frequency of 27 Hz. Plant extracts were incubated at 4 °C shaking continuously for 30 min, centrifuged (15 min, 23 000 g, 4 °C) and split into 4 technical replicates. The H₂O/MeOH phase was transferred to microspine tubes (VWR®, Radnor, Pennsylvania), centrifuged again at 12 000 g for 10 min and the flow-through fraction was evaporated to dryness under gentle stream of nitrogen using a TurboVap® LV evaporation system (Caliper Life Sciences, Hopkinton, MA, USA). Samples were dissolved in 50 µl of 35% methanol and 10 µl was injected onto a reversed-phase column (Kinetex™ C18 100A, 50 x 2.1 mm, 1.7 µm; Phenomenex, Torrance, USA) and analyzed by liquid chromatography–tandem mass spectrometry (LC-MS/MS) using an ACQUITY UPLC® I-Class system combined with a triple quadrupole mass spectrometer Xevo™ TQ-S (Waters, Manchester, UK). The analytes were separated by 9 min linear gradient of 10:90 to 95:5 A:B using 0.1% acetic acid in methanol (A) and 0.1% acetic acid in water (B) as mobile phases at a flow rate of 0.5 ml·min⁻¹ and column temperature of 40 °C. At the end of the gradient, the column was washed with 95% methanol (0.5 min), and re-equilibrated to initial conditions (1.0 min). The effluent was introduced into the MS/MS system with the optimized settings: Source Offset, 60 V; Source Temperature, 150 °C; Desolvation Temperature, 600 °C; Cone Gas Flow, 1000 L·h⁻¹, Collision Gas Flow 0.15 ml·min⁻¹, Nebuliser Gas Flow, 7 Bar; Capillary voltage, 3 kV. For quantification, the multi reaction monitoring (MRM) transitions in positive and negative electrospray modes (ESI⁺ and ESI⁻) were found for each compound as follows: 219 > 161/224 > 163 (ESI⁻), 426 > 246/430 > 250 and 452 > 250/456 > 259 (ESI⁺) for 2,4-D/[²H₅]2,4-D, FluorA I/[¹³C₂]FluorA I and FluorA II/[¹³C₂]FluorA II, respectively. The collision energy and cone voltage were optimized for every transition as well as dwell times for each retention window to obtain a minimum of 15 points per peak. Chromatograms were processed by MassLynx™ V4.1 software (Waters) and quantification was performed by the isotopic dilution method using isotopically labeled standards of each analyte as a reference.

Methods S3 Surface plasmon resonance (SPR).

The experiments were done according to the protocols described in Lee *et al.*, 2014. TIR1 was expressed in *Sf9* insect cell culture using a recombinant baculovirus. The construct contained

sequences for three affinity tags, namely 6 His, maltose-binding protein (MBP) and FLAG. Initial purification using the His tag was followed by clean-up using FLAG chromatography, the purified protein was used for SPR assays by passing it over a streptavidin chip loaded with biotinylated IAA7 degron peptide. The SPR buffer was Hepes-buffered saline with 10 mM Hepes, 3 mM EDTA, 150 mM NaCl and 0.05% Tween 20. Compounds to be tested were premixed with the protein to a final 50 μ M concentration. Binding experiments were run at a flow rate of 30 μ L.min⁻¹ using 3 min of injection time and 2.5 min of dissociation time. Data from a control channel (biotin) and from a buffer-only run were subtracted from each sensogram following the standard double reference subtraction protocol.

Methods S4 GUS assay

Five-day-old *Arabidopsis* seedlings expressing *pDR5::GUS* were treated with 10 μ M fluorescent compounds for 5 h, fixed with ice-cold acetone for 20 min at -20 °C and washed with distilled water three times. Plants were incubated in the presence of GUS staining solution – 2 mM X-GlcA (Duchefa Biochemie) in GUS buffer (0.1% triton X100; 10 mM EDTA; 0.5 mM potassium ferrocyanide; 0.5 mM potassium ferricyanide in 0.1 M phosphate buffer) – at 37 °C in the dark for 30 min. To stop the staining reaction 70 % ethanol was added for 1 h. The samples were then mounted in a mixture of chloral hydrate:glycerol:H₂O (8:3:1) on a glass slide and examined with a Zeiss Axioplan light microscope.

Notes S1 Storage and usage of the compounds.

The FluorA compounds in powder form were kept at 4 °C. Compounds dissolved in DMSO to obtain 1 or 10 mM stock solutions were stored in -20 °C for approx. 2 weeks. Aliquots of the powder were made and dissolved one by one to avoid changing ambient conditions and prevent the compounds from precipitating in DMSO or in water solution of ½ MS medium. Since the solubility of the compounds in water solutions is limited, final concentrations exceeding 10 μ M in liquid medium were not used.

Supplemental references

Eyer L, Vain T, Pařízková B, Oklestkova J, Barbez E, Kozubíková H, Pospíšil T, Wierzbicka R, Kleine-Vehn J, Fránek et al. 2016. 2,4-D and IAA amino acid conjugates show distinct metabolism in *Arabidopsis*. *PLoS One* **11**: e0159269. doi:10.1371/journal.pone.0159269.